Master Thesis of Technical Medicine

3D Printed Moulds for Brachytherapy in Pediatric Head-Neck Rhabdomyosarcomas

August 9, 2024

S.M. Hodes, BSc

Technical Medicine, Track Medical Imaging & Intervention, Clinical Internship M3, Radiotherapy department and 3D-lab, UMC Utrecht

Supervisors

Prof.dr. J.J. Fütterer - Chairman
dr. R. Dávila Fajardo - Medical supervisor, UMCU
H.C. Nguyen, MSc - Technical Medicine, UMCU
C.O. Tan, PhD - Technical supervisor, University of Twente
dr. M. Groenier - Process supervisor, University of Twente
dr. M.L. Groot Koerkamp, PhD - External member, University of Twente

UMC Utrecht

UNIVERSITY OF TWENTE.

Abstract

Rhabdomyosarcoma (RMS) is one of the most common soft tissue sarcomas in children, often affecting the head and neck region. The standard treatment protocol involves a multimodal approach involving systemic chemotherapy, radiotherapy, and potentially surgery. The AMORE procedure replaces external beam radiotherapy with brachytherapy using customized moulds. Despite the benefits of brachytherapy, the current 3D-printed moulds used in the AMORE procedure present limitations. These pre-designed moulds lack the flexibility to adapt to intraoperative changes, often necessitating supplementary materials for a proper fit.

This thesis addresses this limitation of pre-designed 3D-printed moulds by proposing the development of an adjustable mould made exclusively through 3D printing. The new design aims to eliminate the need for supplementary materials while maintaining treatment standards.

A retrospective study was conducted to assess the performance of the current moulds based on dose distribution and fit. This provided a baseline for the development of adjustable moulds. The requirements for these new moulds were formulated based on insights from this study. The design phase involved systematic steps such as mind mapping, morphological overview, and Harris profiles for concept selection. Prototyping determined the final dimensions and margins, and the final designs were tested for compliance with the established requirements.

The results indicate that the new adjustable moulds meet the necessary standards for dose distribution and fit. However, challenges remain in ensuring the robustness of in-vivo assembly and addressing variability in printer output. While the proposed design meets many clinical requirements, further research is needed to refine the materials and methods used, ensure compliance with medical device regulations, and enhance overall reliability.

In conclusion, while the new adjustable moulds represent a promising advancement, further studies are essential to fully realize their potential and ensure they provide consistent, high-quality results.

List of abbreviations

AMORE	Ablative surgery, MOulage afterloading brachytherapy, and surgical Reconstruction
CTV	Clinical Target Volume
EBRT	External Beam Radiotherapy
FLM	Fused Layer Manufacturing
GTV	Gross Tumour Volume
HNRMS	Head-Neck Rhabdomyosarcoma
MDR	Medical Device Regulation
PDR	Pulsed Dose Rate
PEEK	PolyEtherEtherKetone
PTV	Planning Target Volume
RMS	Rhabdomyosarcoma
UMCU	University Medical Center Utrecht

List of Figures

List of Tables

Contents

General introduction

Rhabdomyosarcoma (RMS) is one of the most common soft tissue sarcomas in children. In 40% of the cases, the head-neck region is affected (HNRMS).[1, 5, 6, 7, 8] HNRMS can further be categorized into three distinct anatomical areas: parameningeal, nonparameningeal, and orbit. [6, 7, 8, 9] The prognosis for HNRMS patients is often poor due to delayed diagnosis, partially due to the initial presentation of non-specific symptoms that mimic benign conditions such as allergies or respiratory infections.[9] Diagnostic confirmation of HNRMS is typically achieved through histopathological examination following incisional biopsies.[9, 10] Histologically, RMS can be classified into different subtypes. Embryonal RMS and Alveolar RMS are the most common types observed in the pediatric population.[9, 11, 12]

The standard treatment protocol for RMS involves a multimodal approach, starting with systemic chemotherapy.[1] In order to attain control, local treatment with radiotherapy and potentially surgery is carried out.[1, 6, 8, 10] Microscopic radical resection is often unachievable, especially in parameningeal sites, due to the position and infiltrating nature of the tumour, warranting the use of external beam radiotherapy (EBRT) in the majority of the patients.[5, 6] In 1993, the introduction of the AMORE procedure marked a significant advancement in the treatment protocol.[1, 8] The procedure replaces the use of EBRT with brachytherapy. Brachytherapy creates a more conformal dose delivery with a rapid dose fall-off beyond the target volume, reducing the unnecessary radiation dose to healthy tissues (Figure 1).[1, 5, 6] By limiting exposure to surrounding tissue and accepting microscopic remnants, late side effects are reduced in terms of cosmetic defects and/or functional loss.[5, 8] With the present-day multimodality treatments, long-term survival has increased up to 79-97% in the non-metastatic population, depending on the risk group.[1, 5]

(a) External beam radiotherapy   (b) Brachytherapy
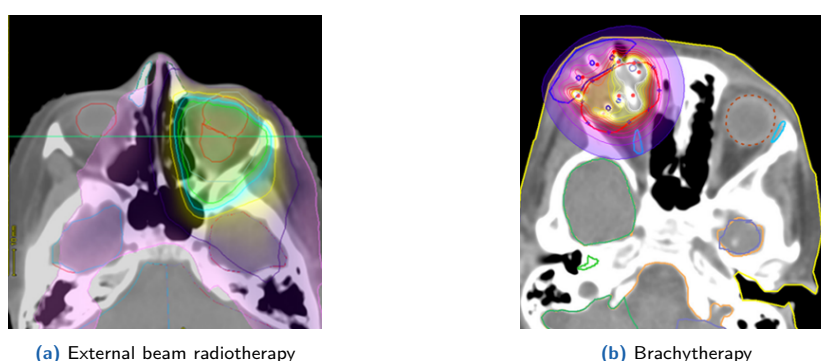
Figure 1: Illustration of external beam radiotherapy and brachytherapy dose distributions of orbital rhabdomyosarcoma. The colored areas represent the isodoses lines of the different dose quantities. Brachytherapy(b) has a much smaller field of irradiation and closer isodoses lines compared to external beam radiotherapy(a). [1]

1.1 AMORE procedure

The acronym AMORE stands for consecutive Ablative surgery, MOulage afterloading brachytherapy, and surgical REconstruction.

Ablative surgery
The initial phase of the AMORE protocol involves a macroscopic resection of the tumour, with the tumour's extent defined based on pre-operative CT/MR imaging.[9] Surgery is executed with a conservative approach, prioritizing the preservation of cosmesis and functionally significant structures such as cranial nerves, blood vessels, bones, and teeth. The possibility of microscopic remnants of the tumour in the wound bed qualifies the site for post-operative brachytherapy as a subsequent treatment step.[9]

MOulage brachytherapy
Moulage brachytherapy aims to deliver an adequate radiation dose to the resection margins to eliminate residual tumour cells while limiting the radiation to healthy tissue.[9] Historically, this was achieved by fashioning a mould from 5 mm thick thermoplastic rubber (gutta percha), cut and layered to the required specifications. Flexible polyethylene catheters were distributed between these layers, typically spaced 5-7 mm apart. This customized mould was then positioned in the surgical bed to facilitate targeted brachytherapy.[6, 9]

The innovation of 3D printing technology has revolutionized this aspect of the AMORE procedure. Starting in 2019, the University Medical Center Utrecht (UMCU) employed 3D printing technology for the design and production of AMORE moulds. This shift was primarily motivated by the unavailability of alternative materials in the market that complied with the Medical Device Regulation (MDR). Additionally, the use of a 3D-printed mould, tailored to the tumour extension on pre-surgical imaging, creates a more accurate fit. This personalized approach also significantly reduces the time required for fitting during surgery when compared to traditional thermoplastics.
Pulsed dose rate (PDR) brachytherapy is delivered with a prescribed physical radiation dose to the clinical target volume (CTV), typically ranging between 40-45 Gy.[6, 9] The dose is administered in 32-36 pulses of 1.25 Gy, with intervals of 2 hours and 6 minutes.[9] Refer to section 1.2 for a more comprehensive explanation of the target volumes, dose volume parameters, the used radionuclide and PDR.

surgical REconstruction
The final stage of the AMORE protocol involves the surgical reconstruction of the wound bed. This process commences approximately one week following the initial ablative surgery. During this second surgery the mould and catheters are carefully removed. Subsequently, a specialized plastic surgeon undertakes the task of reconstructing the surgical defect.[6, 9]

1.2 Brachytherapy

Brachytherapy is a localized cancer treatment method that uses radiation emitted from small, encapsulated radionuclide sources. These sources are strategically positioned in or adjacent to the target area, enabling short-distance radiation delivery.[13] In the context of the AMORE procedure, brachytherapy is implemented through PDR afterloading, employing Iridium-192 (Ir192) as the radiation source.

1.2.1 Target volumes

Effective treatment planning relies on precise delineation of target volumes (Figure 2). The Gross Tumour Volume (GTV) serves as the visible or palpable extent of the tumour, forming the foundation for treatment planning.[14, 2] Subsequently, the CTV expands upon the GTV, encompassing both the demonstrable tumour and microscopic disease extensions at a certain probability level.[14, 2] To accommodate geometric uncertainties, the Planning Target Volume (PTV) incorporates margins around the CTV, ensuring the prescribed dose is delivered despite variations in organ motion and patient setup.[14, 2] In brachytherapy, it is generally assumed that no additional margin is required for either patient-related uncertainties or setup variations. Consequently, the PTV in brachytherapy remains identical to the CTV.[15]
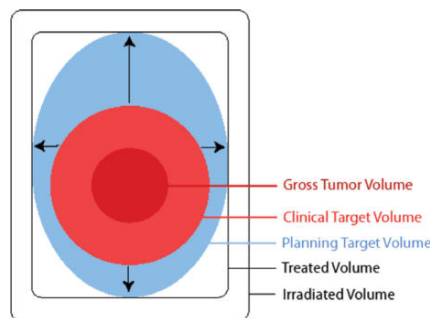
Figure 2: Schematic illustration of the different target volumes. [2]

1.2.2 Dose volume parameters

Dose volume parameters, such as D100% and D90% (the dose delivered to 100% and 90% of the volume respectively), along with metrics like V150%/V200% (the volume receiving 150%/200% of the prescribed dose), are essential for evaluating and comparing treatment plans. These parameters, obtained from dose volume histogram analysis (Figure 3), give a detailed view of dose distribution within the target volume.[16, 3]
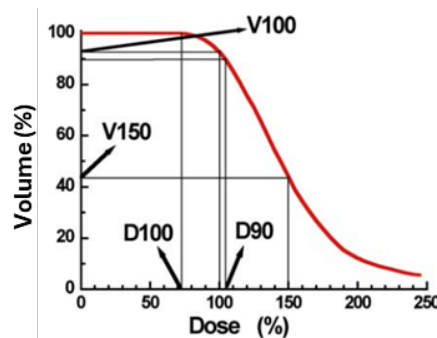
Figure 3: Graphical demonstration of the dose volume parameters based on a dose volume histogram. [3]

1.2.3 Iridium-192

Ir192(1 Ci = 37 GBq) is characterized as a photon-emitting radionuclide, primarily emitting a broad spectrum of γ radiation.[1, 9] It possesses an average photon energy of 0.38 MeV and a half-life of approximately 73.8 days. Additionally, Ir192 has a half value layer in lead of 3 mm.[13]

1.2.4   PDR afterloading

Afterloading is a technique that requires the initial placement of catheters within the treatment area. Subsequently, the radioactive source is introduced through either manual or automatic remote afterloading devices.[13] This source advances through the catheter in increments of 2.5 or 5mm. By finely adjusting the duration of radiation exposure at each position (dwell time), a highly optimized and targeted dose distribution is achieved, enhancing the precision and efficacy of the treatment.[9] The pulsed nature of PDR ensures the feasibility of nursing care and visitations, aspects particularly beneficial in the treatment of young children undergoing the AMORE procedure.[9]

1.3   3D printing

The integration of 3D printing technology into medical practices and innovation is growing, attributed largely to its versatility and accessibility in the market. It offers the advantage of creating patient-specific models that cannot be produced through conventional means.[17] The selection of printing material is highly dependent on the intended application and required certifications. Presently, the brachytherapy department at UMCU uses BioMed Clear for the fabrications of their clinical moulds, while working on the transition to PolyEtherEtherKetone (PEEK).

BioMed Clear resin, printed with the Form 3B 3D printer (Formlabs Inc., USA), is suitable for applications involving prolonged contact with skin and mucosal membranes. It is compatible with all sterilization techniques, enhancing its utility in medical settings. The Formlabs 3B operates with a precision layer thickness up to 50μm.[18] Notably, BioMed Clear adheres to several critical certifications, including USP Class VI and ISO 10993-5, -10, -23, as well as ISO 18562-1, -2, -3, -4, ensuring its compliance with safety and biocompatibility standards.[18]

Since BioMed Clear is only suitable for short-term contact with bone and tissue ($\leq$24 hours), the UMCU aims to transition fully to PEEK for the fabrication of internal moulds, while continuing to use BioMed Clear for external moulds. PEEK is a thermoplastic material known for its lightweight properties and resistance to ionizing radiation.[19] It is printed using the Kumovis R1 printer (3D Systems, USA), a fused deposition modeling printer that processes melted filament, depositing it layer by layer until a three-dimensional component is created (Fused Layer Manufacturing (FLM)).[20] PEEKs compatibility with both tissue and bone makes it suitable for applications directly within open wounds. PEEK meets critical certifications, including USP Class VI and ISO 10993, ensuring its safety for medical applications.[19]

Overhang and bridging
In filament-based 3D printing, each layer is deposited with a certain offset from the previous one, which can be constant or variable. Due to the force of gravity acting on the hot extruded plastic, each deposited strand needs to solidify without drooping or deforming to maintain the intended shape. A key limitation of FLM printing is its disability to print structures where a section of the current layer is not supported by the previous one, known as bridges and overhangs (Figure 4). Overhangs are normally manageable if the angle created by the printing Z-axis is less than 50 degrees. Beyond this threshold, geometrical inaccuracies may occur when not supported.[4]
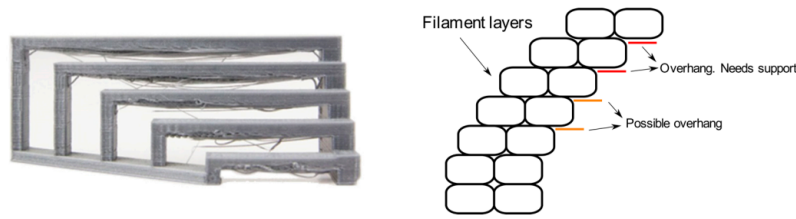
Figure 4: Illustration of the principle of bridging(left) and overhang(right).[4]

1.4   Problem statement

Nowadays the mould is created using 3D printing techniques. However, the introduction of 3D printing of the moulds presented a unique challenge: the reduced adaptability in the operating room. This issue arises due to the pre-designed nature of the 3D-printed moulds, which are tailored based on pre-operative imaging and planning. While these designs aim to accurately represent the tumour geometry, they cannot account for intraoperative changes in the dimension of the resection area. Additionally, they lack the malleability of the thermoplastic material. This rigidity can be a limitation in the dynamic environment of the operating room, where surgeons may need to make real-time adjustments. This can lead to a suboptimal fit, necessitating thermoplastic material attached with wound glue Dermabond as a supplementary resource. However, despite the flexible nature of thermoplastic material, its usage is undesirable due to its time-consuming application and non-compliance with the MDR guidelines. MDR compliance is integral to the responsible development, manufacturing, and use of medical devices, ensuring they are safe, effective, and reliable for patient care.

To address this challenge, a promising solution is the development of an adjustable mould exclusively made with 3D printing. The preferred material would be PEEK, accounting for the imminent transition to this material. The adaptable nature of the new design would eliminate the need for thermoplastic material as a backup. However, it is crucial to ensure that the quality of the treatment process remains unaffected by the new design. Several questions must be addressed to realize this solution: What is the performance of the current mould? How can adaptability be introduced into redesigned moulds? Are the redesigned moulds adequate in terms of dose distribution and fit?

1.5   Objective

The primary objective of this project is:

'Development of an 3D printed adaptable mould, eliminating the need for thermoplastic material while maintaining the current treatment standards'

1.6 Thesis outline

This thesis is structured into six chapters. The **first chapter** serves as the introduction, providing general background information needed for the project. **Chapter two** addresses the research phase. In this phase, a retrospective study is conducted to establish the performance of the current mould. Performance metrics are documented to serve as a baseline that is used during the development of the adaptable mould. The list of requirements for the adaptable mould is covered in the **third chapter**. These requirements are formulated based on the insights gained from the previous chapters. The **fourth chapter** discusses the design phase. It describes the systematic steps taken leading toward the final concept. This includes the utilization of various techniques such as mind mapping, morphological overview, and the application of Harris profiles for concept selection. Prototyping was done to determine the final dimensions and margins of the design. In **chapter five** the final designs were tested for compliance with the previously drawn up requirements. Lastly, **chapter six** engages in discussion and provides recommendations.

2

Research phase - A retrospective study

During the research phase, a retrospective study was executed to provide more insights into the current situation. The analysis included all cases treated at UMC Utrecht from 2019 that utilized 3D-printed moulds for the treatment of HNRMS.

2.1   Introduction

The AMORE procedure is a highly specialized and rare treatment for children with HNRMS, with potential applications in adult care. The UMCU is currently the only center worldwide offering this procedure, with only a few cases performed annually. Consequently, any advancements must be developed internally, with each case playing a crucial role in the iterative refinement and enhancement of the mould design. To support this process, thorough documentation of all changes and enhancements is essential and baseline performance data is needed to assess improvements. However, the current documentation process has been insufficient, with a lack of systematic comparisons between cases. This has led to a limited understanding of the impact of changes over time. This retrospective research aims to address this documentation gap, focusing specifically on performance data related to fit, the need for additional materials, and dose volume parameters. The established data will provide a foundation for further improvements of the mould design.

2.2   Method

This single-centre study retrospectively included 10 patients treated for HNRMS utilizing the AMORE procedure. Patients were included when the treatment used 3D-printed moulds. Pre- and post-surgery CT scans were readily available for all patients.

Data collection involved the use of two software programs: the brachytherapy treatment planning system OncentraBrachy (Elekta Brachytherapy Solutions) (OCB) and Fusion360 (Autodesk). OCB facilitates the segmentation of structures from imaging, catheter placement determination, and dosimetric planning. Fusion can be utilized for further refinement of the model to create a printable mould. Data was collected from both the pre- and post-surgical plans.

OCB
First, a visual inspection of the CT scans was conducted to identify the cases that required extra material in addition to the mould. The location of the corresponding tumour and the nature of the extra material were also reported.

Delineations module

The delineation module in OCB facilitated the extraction of the volume of the mould and any additional material in cubic centimeters (ccm). These volumes were previously segmented by the physician for treatment. When necessary, this segmentation was improved in consultation with the radiotherapy technologist to obtain the most precise volumes.

Planning module

The planning module in OCB facilitates catheter placement and dosimetric planning, enabling the extraction of crucial dose volume parameters for evaluating dose distribution. The parameters under evaluation include the D90%, D98%, V150%, and V200%.

When planning the dose distribution, the aim is to achieve a D90% of 125 cGy in the region surrounding the mould. This region, defined as the CTV minus the mould (Figure 5a), is targeted because it contains the microscopic remnants of the tumour. The dose in the mould itself is not relevant for treatment. Both the D90% and the D98% were extracted for this area.

Additionally, the dose planning aims for the V150% and V200% to be fully inside the mould to prevent excessive radiation to the tissue. Within OCB, two types of V-values are used: $V_{implant}$ and V_{mould}. $V200_{implant}$ refers to the exact volume that receives 200% of the intended dose (the volume within the yellow isodoses line as depicted in Figure 5b), while $V200_{mould}$ refers to the volume of the mould that receives 200% of the intended dose. When these volumes are the same, it indicates that the entire 200% dose is contained within the mould. The same principle applies to the $V150_{implant}$ and $V150_{mould}$. The percentage that is not contained within the mould could be calculated using the formula $\frac{V_{implant} - V_{mould}}{V_{implant}} \cdot 100\%$.

(a) Delineations
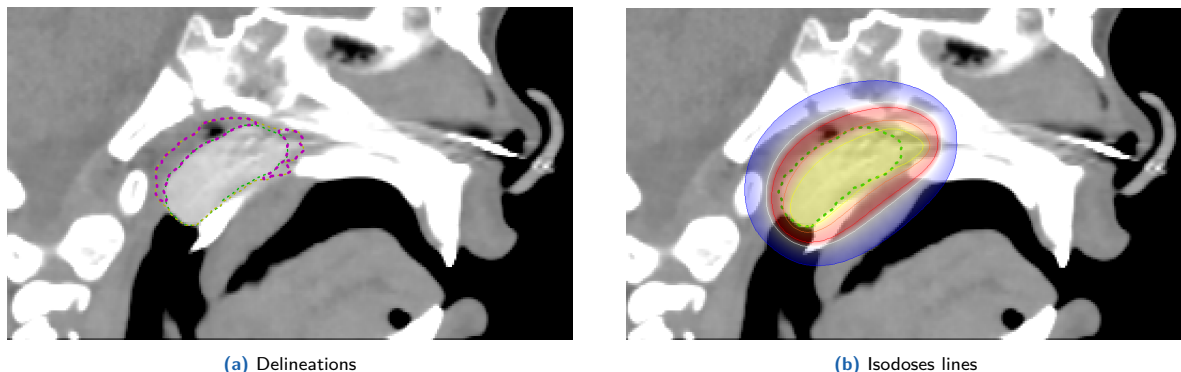
(b) Isodoses lines

Figure 5: Illustration of an implanted nasopharynx mould. (a) shows the different delineations; dotted green=mould, dotted yellow=CTV, dotted pink=CTV-mould. (b) shows the isodoses lines of the catheters within the mould(green dotted line); yellow=V200%, orange=V150%, red=V100%

Fusion

The exact volumes of the models that were printed and used in the surgery were extracted from Fusion, allowing for a direct comparison with the implanted volumes obtained from OCB.

2.3 Results

Based on the visual inspection, it was determined that 70% of the cases required some form of additional material (Figure 6a). Among the ten cases, six were situated in the parameningeal area, three in the orbit, and one in the non-parameningeal area. Notably, the orbit exhibited the highest success rate in terms of fit, with 66% of cases not requiring extra material.

Figure 6b provides a more detailed differentiation between used materials. In four cases (57.1%), thermoplastic material was employed, while gauze was used in two cases (28.6%), and silicone in one case (14.3%). In six cases, the extra material also served as a medium for additional catheters, predominantly in cases involving thermoplastics or silicone.
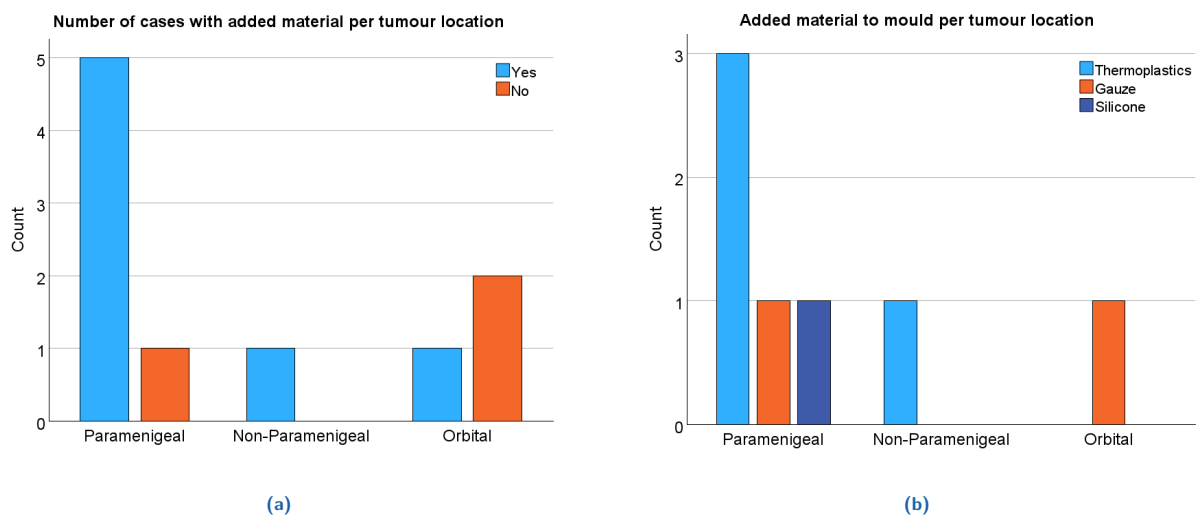
Figure 6: Analysis of the use of extra material in addition to the printed mould. The histogram in *(a)* groups the cases based on the need for extra material and *(b)* provides a more detailed breakdown of the source of the extra material.

Volumetric data

In nearly all cases, the total implanted volume (including both the mould and the added material) is equal to or greater than the printed volume generated in Fusion. Figure 7 illustrates these volumes plotted against each other, with the line representing $x = y$ (indicating an equal relationship). An exception is observed in number 7, where the printed mould is notably larger than the implanted volume. Although number 1 might initially appear to be the anomaly, the implanted volume still exceeds the printed volume, consistent with the other cases.

Dosimetric data

The mean D90% is calculated at 125 cGy, reaching the target of 125 cGy. Meanwhile, the mean D98% registers at 110.8 cGy. Notably, the mean percentage of V200% lying outside the mould is recorded at 15.8%, whereas V150% exhibits a mean of 22.1%. These parameters are graphically represented by boxplots in Figure 8a and 8b, with detailed values provided in Appendix A.1.
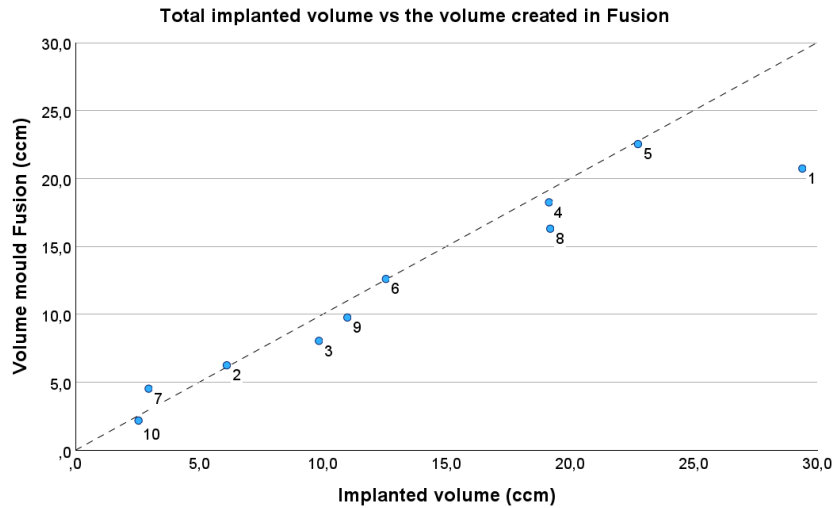
Figure 7: The total implanted volume plotted against the 3D-printed volume created in Fusion. Each dot represents a different clinical case, the line represents $x = y$. Numbers 2, 5 and 6 represent cases where the total implanted volume is equal to the volume generated in Fusion. Numbers 1, 3, 4, 8-10 represent cases where the total implanted volume is greater than the volume generated in Fusion. Number 7 represents an irregularity where the total implanted volume is smaller than the volume generated in Fusion.
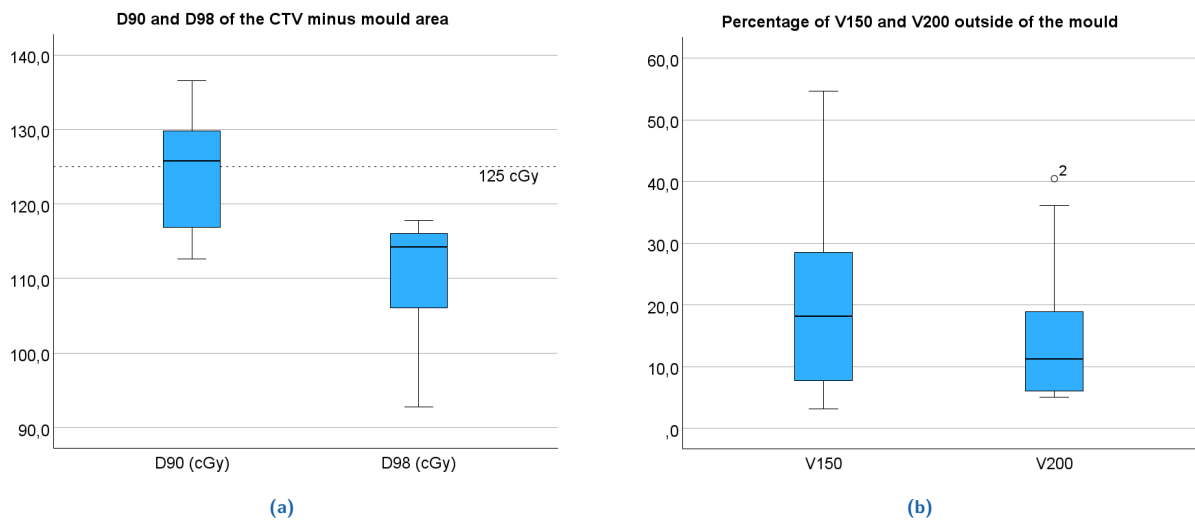
Figure 8: *(a)* Boxplot of the D90% and D98% values (the dotted line represents the aimed dose of 125 Gy for D90%) and *(b)* boxplot of the V150% and V200% values

2.4 Discussion

This study conducted a global analysis of 10 cases undergoing the AMORE procedure using 3D-printed moulds. The key findings of the study include:

- In the majority of cases, additional materials were required to expand the mould.

- Introduction of materials other than gauze necessitated the placement of extra catheters.

- The objective of achieving D90%$\geq$125Gy was successfully met.

- The mould did not achieve complete coverage of V150% and V200%.

In assessing the overall fit of the moulds, the orbital mould demonstrated superior results compared to other locations based on the need for additional material. However, it is noteworthy that the orbital area benefits from distinct boundaries provided by bony structures, aiding in mould design by offering clear borders. Unlike bone, soft tissue in other anatomical areas can be subjected to extra removal due to suspicion of tumour cells. Moreover, the presence of three cases in this exact location suggests the development of a standardized mould creation approach. In contrast, the other cases are all in different locations and lack bony structure encasement. This requires the development of an entirely new mould design each time with little standardisation. This discrepancy underscores the challenges associated with mould creation in diverse anatomical regions.

The anticipated volumes of the total implant are expected to be equal to or larger than the printed mould, as either the printed mould is implanted directly, or extra material is added during the procedure. However, an exception to this hypothesis is evident in case number 7. Upon reviewing the surgical reports, it is apparent that case number 7 required extensive shaping, with significant shaving of the mould during the operation to ensure proper fit. Consequently, in this particular case, the actual implant volume is considerably smaller than the printed volume. This highlights the variability that can be encountered during the implantation process.

Additionally, there is a discrepancy in precision between volumes obtained from segmentation and those extracted from Fusion. Fusion provides the volume of the exact model, whereas segmentation from scans introduces potential observer errors and errors due to scan quality variations. Consequently, volumes derived from segmentation are inherently less precise, introducing some degree of deviation when compared to the exact volumes extracted from Fusion. The segmentations involve relatively small volumes, which might amplify the impact of any errors in relation to the total volume. Additionally, a discrepancy arises in the inclusion of catheter paths within the total volume during segmentation, whereas these paths are excluded from the volume when extracting the model from Fusion.

Upon analysis of the dose volume parameters, it is evident that the targeted D90% at 125 cGy is successfully delivered. However, when assessing V200%, a notable percentage of the volume lies outside the mould. Visual analysis of the dose plans reveals that all of this volume outside the mould is in air, which lessens the impact of this percentage. Similarly, for V150%, the majority of the volume that lies outside the mould is located in air, with minimal presence in tissue. In the planning process, concessions are sometimes necessary to ensure the delivery of the desired dose.

In conclusion, this study has provided the desired insights into the current status of the moulds used in the AMORE procedure. It has provided valuable documentation of the current baseline characteristics of the moulds. These characteristics can be used in further development aimed at optimizing mould design.

3

Requirements

In this chapter, the list of requirements is established. These requirements serve as fundamental guidelines and criteria for the development and evaluation of the proposed solutions. The MoSCoW method was used to prioritize the requirements. This is a systematic approach that categorizes requirements into four distinct groups: Must have, Should have, Could have, and Won't have.[21]

	Requirement	MoSCoW
1	**Material**	
1.1	The mould is printed using PEEK	S
1.2	The mould can be used without Dermabond	S
2	**3D-print**	
2.1	The mould is based on CT/MR imaging of the tumour	M
2.2	The mould is smooth	S
2.3	The mould is stable when implanted and can withstand a force up to 30N	M
2.4	The 3D-print is reproducible	M
2.5	The catheter paths are permeable	M
3	**Dose distribution**	
3.1	The total mould captures the V200%	M
3.2	The total mould captures the V150%	S
3.3	The D90%/D98% values of the CTV-mould are at least equal to the current plan	S
4	**Fit**	
4.1	The size of the mould is adjustable	M
4.2	The mould can be adjusted to fit the resected area within 30 minutes	S
4.3	Assembly of the mould is possible in-vivo	C

1. Material

The first set of requirements describes the specifications for the materials employed in the mould process. It is desired that the mould is constructed from the biocompatible and 3D-printable material PEEK, keeping the aspired transition to this material in mind. Additionally, it is preferred to avoid using the wound glue Dermabond for the assembly of the mould. Instead, an alternative coupling system is recommended.

2. 3D-print

The second set of requirements describes various aspects related to the 3D print. Firstly, the design of the print is crafted based on the delineations of the CTV from CT/MR imaging. Secondly, the mould should be smooth. If a print were made with the Kumovis R1 printer, high printing temperatures could result in melting of the outline of the mould, causing inconsistencies in the outer layer. Additionally, increased discomfort to the patient would be prevented. Third, the mould must be constructed in a firm manner as it is imperative that it does not break apart during placement. The choice of 30 N is based on the strongest maximum pinch strength, which is 87 N for males in their forties and 58 N for females in their twenties. [22] It is estimated that the force applied to the mould during use in the operating room will not exceed half the maximum strength of females. The mould also must be reproducible for testing pre-surgery and as backup during surgery. Furthermore, the catheter paths must be designed to accommodate 6 Fr catheters, positioned in diverse configurations.

3. Dose distribution

The core of the mould is subjected to very high doses of radiation. To minimize tissue damage, it is of importance that the volume of V200% remains contained within the mould. Similarly, while containment of V150% is also crucial, its impact is slightly less significant due to its lower damaging potential. Results from the retrospective study indicated that the D90% and D98% values of the current mould consistently met the desired thresholds. Therefore, the new mould must at least achieve these dosimetric values.

4. Fit

In order to achieve the desired flexibility during surgery, it is essential that the size of the mould can be easily adjusted. However, any prolongation of the current operating time is not desired. Additionally, the possibility of in-vivo assembly of the mould would be beneficial.

4

Design phase

In this chapter, the design phase was initiated, using the insights gained from the research phase *(chapter 2)* and the formulated requirements *(chapter 3)*. The design phase contains several sections, beginning with idea generation. Mindmaps outlining various features were created to generate ideas. These ideas were then combined into morphological overviews, which were used to create concepts. The final concept was selected using Harris profiles to facilitate decision-making. The chapter concludes with prototyping, where the final concept was implemented in a clinical case.

4.1   Idea generation

Mindmaps are considered a useful and simple method for rapidly generating structured ideas. In the center of the generated mindmaps are the features for which design freedom has been established: shape adaptation and coupling mechanisms. When considering all requirements, these two features allow for alterations that could introduce adaptability to the mould. Once these features were identified, ideas and associations were added to each feature, serving as inspiration for the attributes incorporated into the morphological schemes of the next chapter.
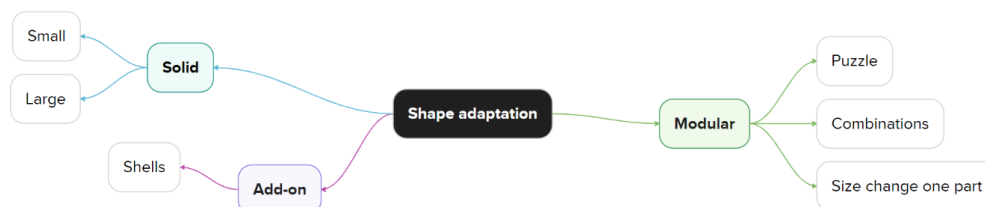
Figure 9: Mindmap for the idea generation of possible solutions for the feature shape adaptation.
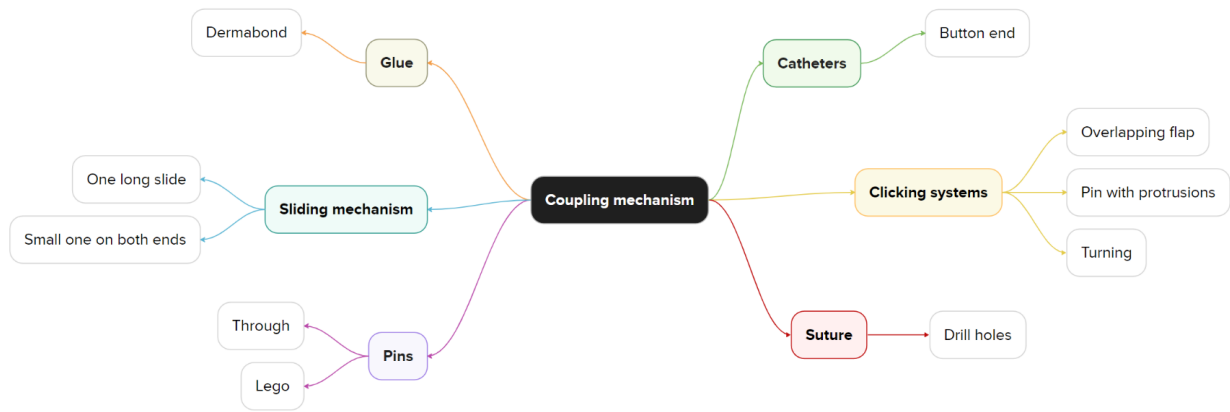
Figure 10: Mindmap for the idea generation of possible solutions for the feature coupling mechanism.

4.2 Morphological overview

Two morphological overviews were created to generate concepts derived from the mindmaps. Both overviews incorporated the features of "shape adaptation" and "coupling mechanism". The Kumovis R1 printer introduces several restrictions related to the printing direction. Due to printing limitations related to overhang and bridging, the catheter paths must be printed perpendicular to the printing table. Additionally, these factors affect the feasibility of some ideas for the feature 'coupling mechanism'. Therefore, a distinction was made based on the orientation of the assembling plane relative to the direction of the catheter paths. One overview was developed for the assembling plane parallel to the catheter paths (Table 1), while the other was designed for the assembling plane perpendicular to the catheter paths (Table 2).Therefore, a distinction was made based on the orientation of the assembling plane relative to the direction of the catheter paths. One overview was developed for the assembling plane parallel to the catheter paths (Table 1), while the other was designed for the assembling plane perpendicular to the catheter paths (Table 2). Both orientations are necessary to ensure that the mould can be adapted to meet the specific needs of different patients.

Shape adaptation
Several methods for shape adaptation were proposed to facilitate adaptability. First, the mould can be printed as a single unit, available in various sizes and shapes. An alternative approach involves printing a base mould with optional, shell-like add-ons, allowing for customization based on change. Last, a modular mould is considered, dividing the mould into separate segments, each printed in different sizes. This segmentation allows for the combination of segments in different configurations, enabling adjustments to specific areas of the mould.

Coupling mechanism
Several options were explored for coupling the different mould components. The coupling mechanism is differentiated based on whether the assembling plane is parallel or perpendicular to the catheter paths, as this significantly impacts the feasibility of printing.

Parallel:
Glue, Pinning mechanism, Drilling holes to attach the segments with sutures, Sliding mechanism
Perpendicular:
Glue, Pinning mechanism, Drilling holes to attach the segments with sutures, Catheters to fixate both parts, Overlapping 'clicking' system, The lock-insert system

Table 1: Morphological overview with possible solutions for the features shape adaptation and coupling mechanism, relating to the assembling plane parallel to the catheters .

Table 2: Morphological overview with possible solutions for the features shape adaptation and coupling mechanism, relating to the assembling plane perpendicular to the catheters .

4.3   Concept generation

By combining the various attributes of the two features, the most promising concepts were generated. This section provides a detailed overview of these concepts, discussing their positive and negative attributes.

4.3.1   Concepts parallel

Table 3: Most promising combinations from the morphological overview with the assembling plane parallel to the catheters.

16

Concept 1 - Blue

Concept Blue combines the printing of a basic mould with add-ons, coupled together using a pinning mechanism. This mechanism offers easy assembly and disassembly. However, extensive testing is required to determine the appropriate margins and dimensions to ensure a secure fit of the pins. Moreover, printing pins in the parallel direction can pose challenges due to overhang and bridging when using the Kumovis printer. Additionally, the feasibility of printing add-ons may be limited by their small size, leaving less room for implementing a coupling mechanism, affecting the connection strength. Depending on the dimensions of the pins, in-vivo assembly may be feasible.

Concept 2 - Orange

Concept Orange combines the printing of a basic mould with add-ons, coupled with sutures for assembly. Suturing requires small holes to be drilled into the mould, which may pose challenges given the shell-like nature of the add-on concept. The feasibility of printing add-ons may be limited by their small size, leaving less room for implementing a coupling mechanism. Additionally, suturing as a coupling mechanism is more time-consuming, as sutures need to be cut and reapplied when switching sizes. In-vivo assembly would not be possible using this method. Additionally, the presence of sutures and knots on the exterior may result in a less smooth surface. Nevertheless, the connection strength is robust due to the strength of the sutures.

Concept 3 - Dark green
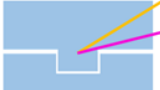
Concept Dark green involves printing the mould in segments and coupling them with a pinning mechanism. Printing in segments offers the advantage of creating larger parts compared to printing with add-ons. A pinning mechanism facilitates easy assembly and disassembly; however, thorough testing is required to ensure proper fit and dimensions of the pins. Challenges may arise in printing pins in the parallel direction due to overhang and bridging when using the Kumovis printer.

Concept 4 - Red

Concept Red combines printing the mould in segments and coupling them with a sliding mechanism. Printing in segments offers the advantage of creating larger parts compared to printing with add-ons. A sliding mechanism provides ease of assembly and disassembly; however, thorough testing is necessary to ensure the mechanism fits tightly enough. In the parallel direction, a sliding mechanism is easier to print since there are no overhangs or bridging concerns.

4.3.2   Concepts perpendicular

Table 4: Most promising combinations from the morphological overview with the assembling plane perpendicular to the catheters.

Concept 1 - Yellow

Concept Yellow integrates the printing of a basic mould with add-ons, coupled with a pinning mechanism for assembly. Pinning mechanisms offer easy assembly and disassembly, although extensive testing is required to ensure proper fit of the pins. Moreover, in the perpendicular direction, printing pins is straightforward as there are no concerns about overhang or bridging. However, the feasibility of printing add-ons may be limited due to their small size, which also restricts the implementation and dimensions of coupling mechanisms, affecting the connection strength. Depending on the dimensions of the pins, in-vivo assembly may be possible.

Concept 2 - Pink

Concept Pink involves printing the mould in segments and coupling them with a pinning mechanism. Printing in segments offers the advantage of creating larger parts compared to printing with add-ons. A pinning mechanism provides easy assembly and disassembly; however, thorough testing is required to ensure proper fitting of the pins. Additionally, in the perpendicular direction, printing the pins is straightforward as there are no concerns about overhang or bridging.

Concept 3 - Lime green

Concept Lime green entails printing the mould in segments and coupling them with sutures. Printing in segments offers the advantage of creating larger parts compared to printing with add-ons. However, to apply the sutures, small holes must be drilled into the mould. The application of sutures as a coupling mechanism is more time-consuming, as sutures need to be cut and reapplied when switching sizes. Furthermore, assembly using sutures will not be possible in-vivo. Additionally, the exterior surface may be less smooth due to the presence of sutures and knots. Nevertheless, the connection strength is favourable due to the properties of the sutures.

Concept 4 - Purple

Concept Purple involves printing the mould in segments and coupling them with a catheter. Printing in segments offers the advantage of creating larger parts compared to printing with add-ons. Fixation with catheters is achievable by utilizing existing catheter paths and securing the catheters at the end with a button. However, this fixation method requires significant space within or outside the mould. Additionally, using a round button for fixation, which is 10 mm in diameter, may be too large in comparison to the mould itself and may not always fit into the created wound. Moreover, assembly in-vivo would pose challenges.

4.4 Concept selection

All concepts were evaluated to select two final design concepts (one for each orientation) for further development. Objective concept evaluation was conducted using Harris profiles. Five features were established for analysis:

1. Speed: Would the mould be easy and fast to use in the operating room?
2. Surface: How uniform would the resulting mould surface be?
3. Printability: Would both printers in the UMCU be able to print the design?
4. Connection strength: How strong would the mould be?
5. In-vivo assembly: Would it be possible to assemble the mould in-vivo?

Each concept was scored -2, -1, 1, or 2 points for each criterion. The designs with the highest overall score were chosen for further development. The Harris profiles can be found in Table 5 and 6.

Table 5: Harris profiles for the concepts regarding the assembling plane parallel to the catheters

	Blue				Orange				Dark green				Red			
	-2	-1	1	2	-2	-1	1	2	-2	-1	1	2	-2	-1	1	2
Speed			green	green	red	red					green	green			green	green
Surface		red				red				green					green	
Printable	red	red			red					red					green	green
Connectivity			green	green			green				green	green			green	green
Multi-usability			green			red					green				green	
Assembly in-vivo		red			red	red				red				red		
Total	1				-6				4				7			

The selected concept for the adaptable mould utilizing a assembling plane parallel to the catheters is Concept Red. This concept incorporates a modular build for the mould, coupled with a sliding mechanism as the coupling system. In the next chapter, the testing phase will examine the precise printing features of this concept.

Table 6: Harris profiles for the concepts regarding the assembling plane perpendicular to the catheters

	Yellow				Pink				Lime Green				Purple			
	-2	-1	1	2	-2	-1	1	2	-2	-1	1	2	-2	-1	1	2
Speed			green	green			green	green	red	red					green	green
Surface		red					green			red					green	
Printable	red	red					green				green	green			green	green
Connectivity			green	green			green	green			green			red		
Multi-usability			green							red						
Assembly in-vivo		red				red			red	red				red		
Total	1				6				-3				2			

The selected concept for the adaptable mould utilizing a assembling plane perpendicular to the catheters is Concept Pink. This concept incorporates a modular build for the mould, coupled with a pinning mechanism as the coupling system. In the next chapter, the testing phase will explore the precise printing features.

4.5 Prototyping

Prototype testing was done to determine the optimal dimensions and margins for the 3D-printed joint mechanisms. Prototypes of the chosen designs were produced using the available Form 3B printer with Biomed Clear resin. Once the dimensions and margins were established using test cubes, the mechanisms were implemented in a clinical case from the retrospective study, specifically involving a tumour in the parapharyngeal space/masticator space on the left side. A comprehensive overview of all conducted tests can be found in Appendix A.2.

4.5.1 Sliding mechanism

The sliding mechanism consists of two main components: the protruding part and the corresponding slot. Figure 11a illustrates the design of the protruding part along with the implementation in the clinical case. The base length is 4 mm, the top length is 6 mm, and the height is 2 mm. The upper edges are rounded with a radius of 0.5 mm. The ideal margin was determined to be 0.15 mm for the mechanism and 0.1 mm between the cutting planes. The design of the entire mechanism includes two joints positioned on opposite ends of the cutting plane, with their configurations mirrored. Each joint is 5 mm in length.

4.5.2 Pinning mechanism

The pinning mechanism features a slightly tapered pin, designed with a lower diameter of 2.8 mm and an upper diameter of 2.6 mm. The top of the pin is rounded with a radius of 0.5 mm. This pin fits into a hole with a diameter of 2.8 mm, incorporating a 0.05 mm margin to ensure proper fit. Figure 11b illustrates the tapered pin along with the implementation in the clinical case.

(a)   (b)
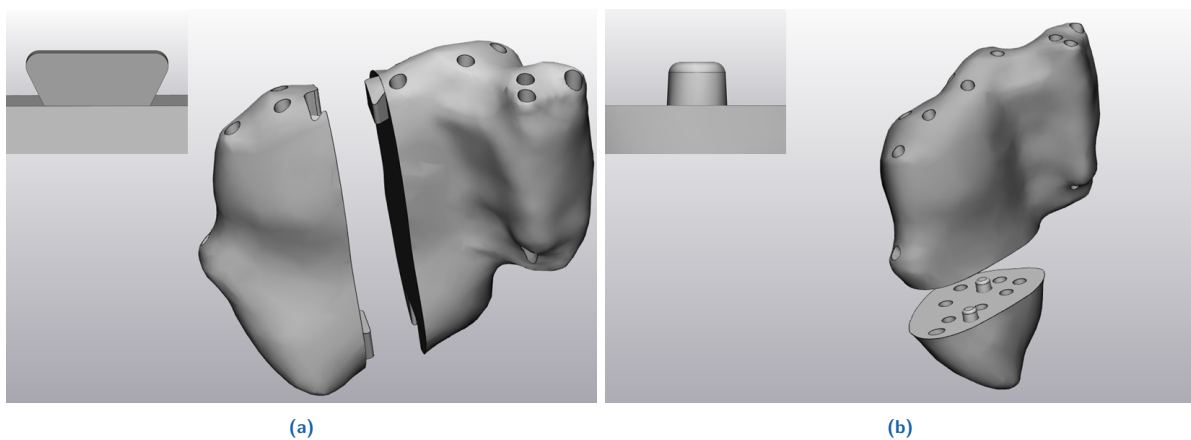
Figure 11: Illustrations of the coupling mechanism. *(a)* shows the protruding part of the sliding mechanism and *(c)* shows the tapered pinning mechanism.

5

Testing phase

This chapter outlines the testing phase, during which the implemented concepts were assessed against the previously established requirements. Six tests were conducted, each corresponding to specific requirements. Prior to the tests, the moulds were sterilized by the Central Sterilization Department to mimic clinical conditions.

5.1 Method

5.1.1 Reproducibility and mould stability

To test if the mould is reproducible, taking requirement *2.4: The 3D-print is reproducible* into consideration, the final mould designs were printed twice. All prints were made using the same printing configurations. Consistent performance across both moulds would demonstrate reproducibility.

To ensure the strength of the coupling mechanisms per requirement *2.3: The mould is stable when implanted and can withstand a force up to 30 N*, testing was conducted using manual and digital Newton meters (Figure 12). Initially, the moulds were subjectively evaluated by assembling/dissembling to assess if the connection felt tight or loose. This served as an initial judgment of reproducibility. The stability of the mould was then evaluated based on two factors. First, the mechanical strength of the coupling mechanism was assessed to confirm it would not break during handling in the operating room. Second, the integrity of the connection was tested to prevent unintentional disassembly during implantation. Both factors were tested for all possible segment combinations within the two prints.

(a)

(b)

Figure 12: *(a)* digital Newton meter and *(b)* manual Newton meters of 100, 300, 600 and 2500 gram.

The mechanism's strength was tested by placing one half of the mould in a vise. A digital Newton meter was then attached to the other half using fishing wire. With the Newton meter in place, a force of up to 30 N was applied perpendicular to the coupling mechanism. Refer to Figure 13 for the exact setup.

(a)

(b)
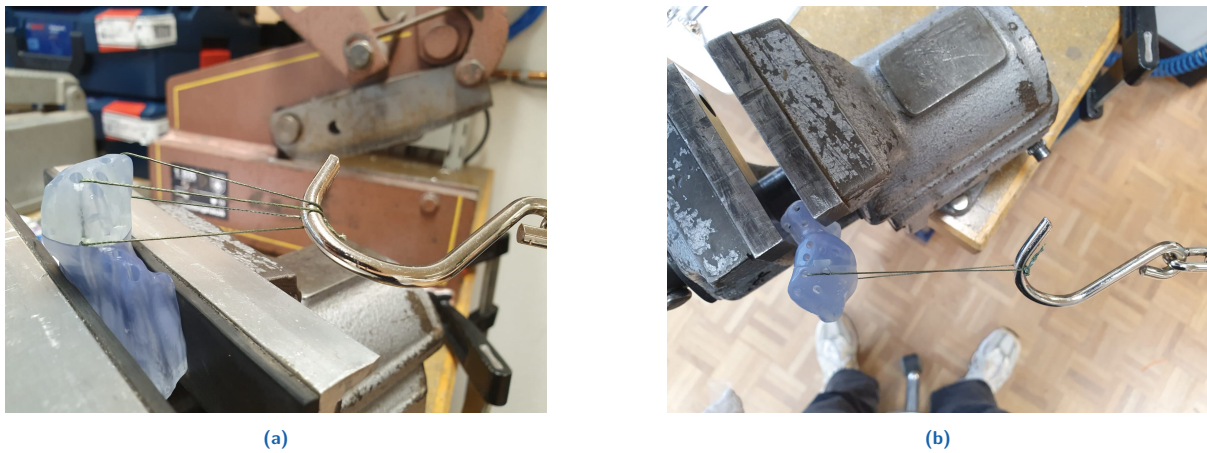
Figure 13: Graphic representation of the test setup to assess the strength of the coupling mechanisms by pulling perpendicular. *(a)* shows the setup for the pinning mechanism and *(b)* shows the setup for the sliding mechanism.

The firmness of the connection was tested by placing one half of the mould into a vise. A manual Newton meter was then attached to the other half using fishing wire. The strength of the used Newton meter depended on how firm the connection was. With the Newton meter in place, force was applied until the mould would dissemble. Refer to Figure 14 for the exact setup. A force of 10 N was used as criterion for this part of the experiment, based on the force it takes to pull a fixed catheter loose as measured by the UMCU.

(a)

(b)
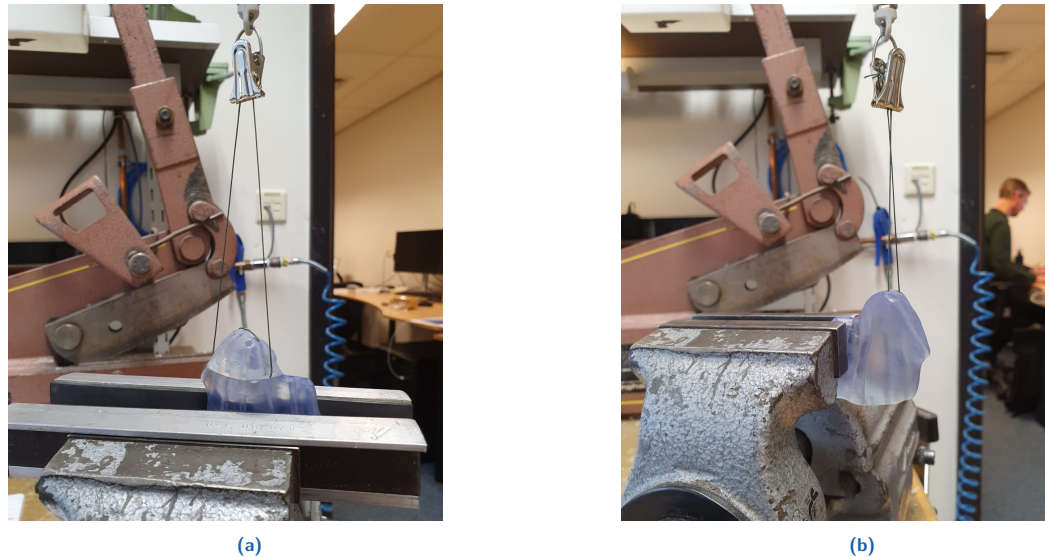
Figure 14: Graphic representation of the test setup to assess the firmness of the connection by pulling parallel to the coupling mechanism. *(a)* shows the setup for the pinning mechanism and *(b)* shows the setup for the sliding mechanism.

5.1.2 Mould appearance

To assess the surface texture of the moulds per requirement *2.2: The mould is smooth*, a thorough evaluation was conducted using both visual inspection and tactile examination. The presence of any sharp protrusions or inconsistencies in the outer layer was carefully noted.

5.1.3 Permeability

Accessibility testing was conducted to verify the permeability of catheter paths in accordance with requirement *2.5: the catheter paths are permeable*. First, catheters were inserted in the paths to manually check the passage. The accessibility testing method, already employed for clinically used moulds, involved creating a simple dose plan and loading it into the radiation system. The plan consisted of 11 pulses, with each pulse applied to a different catheter path (Figure 15) within the mould. The absence of errors during the plan execution would indicate that the mould passed the accessibility test, confirming its safety for clinical use.
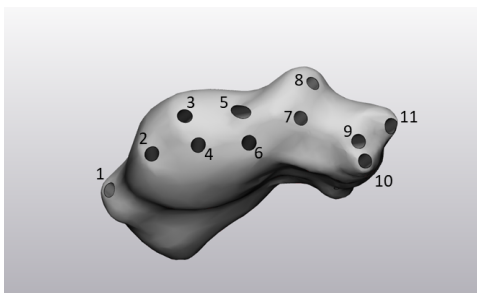
Figure 15: The numeration used for the catheter paths.

5.1.4 Dose volume parameters

In silico testing was performed to determine dose volume parameter values per requirements *3.1: The total mould captures the V200%*, *3.2: The total mould captures the V150%* and *3.3: The D90%/D98% values of the CTV-mould are at least equal to the current plan*.

First, a CT scan of the new mould had to be obtained. To replicate clinical conditions, the mould was placed in water and the slice thickness was set to 1 mm. The CT scan was then loaded into the matching module of the OCB software. Point registration was performed using the beginning and end of the catheter paths to align the new mould with the existing one. In the delineation's module, the new mould was delineated, and this delineation was subsequently loaded into the planning module using the dose plan of the existing mould. To extract the V150%, V200%, D90%, and D98% values of the new mould design, the method described in Section 2.2 was employed. This ensured a consistent approach for comparing dose distributions.

5.1.5 Remaining requirements

The factual requirements *1.1: the mould is printed using PEEK, 1.2: the mould can be used without Dermabond, 2.1: the mould is based on CT/MR imaging of the tumour, 4.1: the size of the mould is adjustable* and *4.2: the mould can be adjusted to fit the resected area within 30 minutes* were evaluated on a PASS/FAIL basis to confirm compliance.

5.2 Results

5.2.1 Reproducibility and mould stability

During the preliminary assessment of the moulds, it already became apparent that the tightness of the sliding mechanism differed depending on the combination of segments. The segments related to the pinning mechanism all felt adequate.

All segment combinations of the mould printed with the pinning mechanism could withstand a perpendicular force of 30 N without any instances of breakage. The force required to disassemble the connection ranged from a minimum of 1.4 N to a maximum of 8.3 N, with a median of 3.95 N. A more detailed description of the results is provided in Table 7.

Table 7: Results of the test conducted on the mould design with pinning mechanism regarding the strength and firmness of the connection

Pinning mechanism

Mechanism strength

	Holds 30 N	Max tested		Holds 30 N	Max tested
1+3	✓	30 N	2+3	✓	30 N
1+4	✓	30 N	2+4	✓	30 N
1+5	✓	30 N	2+5	✓	30 N
1+6	✓	30 N	2+6	✓	30 N

Firmness connection

	Force (g)	Force (N)		Force (g)	Force (N)
1+3	850	8.3	2+3	610	6.0
1+4	410	4.0	2+4	400	3.9
1+5	210	2.1	2+5	140	1.4
1+6	150	1.5	2+6	440	4.3
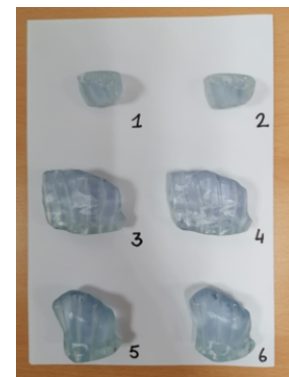
All segement combinations of the mould printed with the sliding mechanism could withstand a perpendicular force of 30 N without any instances of breakage. The force required to disassemble the connection ranged from a minimum of 0.2 N to a maximum of 10.8 N, with a median of 1.45 N. A more detailed description of the results is provided in Table 8.

Table 8: Results of the test conducted on the mould design with sliding mechanism regarding the strength and firmness of the connection

Sliding mechanism

Mechanism strength

	Holds 30 N	Max tested		Holds 30 N	Max tested
a+c	✓	50 N	b+c	✓	50 N
a+d	✓	50 N	b+d	✓	50 N
a+e	✓	50 N	b+e	✓	50 N
a+f	✓	50 N	b+f	✓	50 N

Firmness connection

	Force (g)	Force (N)		Force (g)	Force (N)
a+c	23	0.2	b+c	22	0.2
a+d	24	0.2	b+d	180	1.8
a+e	1050	10.3	b+e	1100	10.8
a+f	110	1.1	b+f	245	2.4
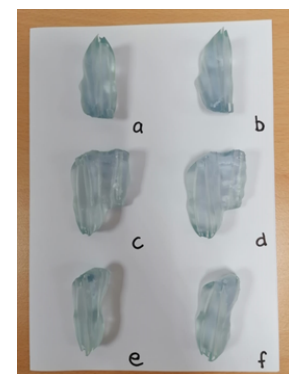
Due to a possible error in equality of the used print configurations, a second set was printed for the mould with the sliding mechanism. These reprints could also withstand a perpendicular force of 30 N without any instances of breakage. The force required to disassemble the connection ranged from a minimum of 0.2 N to a maximum of 22.6 N, with a median of 2.95 N. The exact results of this reprint can be found in Appendix A.3

5.2.2 Mould appearance

Upon tactile examination, it was observed that certain combinations of segments had noticeable edge on the transition of the cutting planes. These inconsistencies were evident in combinations where an original mould segment was joined with the larger segment.

5.2.3 Permeability

During the initial catheter insertion check, no obstructions were found within the catheter paths. The subsequent accessibility tests confirmed that all paths were permeable and suitable for the delivery of PDR brachytherapy.

5.2.4 Dose volume parameters

The adaptable mould exhibits D90% and D98% values calculated at 124.1 cGy and 111.6 cGy, respectively, slightly below those of the current mould (124.7 cGy and 111.8 cGy). Additionally, the percentages of V150% and V200% outside the mould are determined to be 21.5% and 13.5%, respectively, also slightly lower compared to the current mould (22.8% and 13.6%). Table 9 provides an overview of these results.

Table 9: Dose volume parameters of both the current and adaptable mould in the same patient, calculated using an identical dosimetric plan

	D90% (cGy)	D98% (cGy)	V150% outside mould (%)	V200% outside mould (%)
Current mould	124.7	111.8	22.8%	13.6%
Adaptable mould	124.1	111.6	21.5%	13.5%

5.2.5 Remaining requirements

Three out of five requirements were labeled with a PASS. One requirement partially passed (*1.2: The mould can be used without Dermabond*) and one requirement failed (*1.1: The mould is printed using PEEK*). A more detailed description of the results can be found in Table 10.

Table 10: Detailed description of the PASS/FAIL requirements

1.1	The mould is printed using PEEK	FAIL	The mould is printed using BioMed Clear resin due to technical difficulties with the Kumovis printer
1.2	The mould can be used without Dermabond	PASS/FAIL	It is possible to use the mould without Dermabond. However, in practice Dermabond is still used to fixate the catheter ends
2.1	The mould is based on CT/MR imaging of the tumour	PASS	The mould is made based on CT imaging
4.1	The size of the mould is adjustable	PASS	The modular nature of the mould makes it adjustable
4.2	The mould can be adjusted to fit the resected area within 30 minutes	PASS	The swapping of the segments takes less than 30 minutes

6

Discussion and recommendations

This thesis investigated the development of an adaptable mould exclusively made with 3D printing techniques, which would eliminate the need for thermoplastic material while maintaining the current treatment standards. Two mould designs were created, depending on the orientation of the cutting plane relative to the direction of the catheter paths.

The proposed method showed significant variation in the tightness of the sliding mechanisms when combining different segments. The required force to disassemble the moulds ranged from 0.2 to 10.8 N. These inconsistent and diverse values indicated that most combinations were not tight enough and that the mould was not reproducible. Although the pinning mechanism performed slightly better, it still did not meet the requirements. The issues stem from printer variability. Given the small margins, even minor print variations can significantly affect the fit. Increasing the size of the coupling mechanism could reduce this problem, but this is not feasible due to the size of the mould and included catheter paths.

Consultations with radiotherapists revealed that a loose mechanism is not critical. Since Dermabond is already used to fixate the catheter ends to the mould, a small drop can also be applied to secure the segments. Additionally, the pressure from surrounding tissue in the wound bed would keep the mould together. Given the optional use of Dermabond, the margin of the coupling mechanism could be increased, mitigating the impact of the printer variability. This would result in a mechanism that still only has one degree of freedom and is considered reproducible.

Some surface variability was observed during the tactile examination of the moulds. This variability occurred at the transition points between several segments, resulting in slight edges. Although these transitions were barely perceptible to the touch, they can be easily addressed through post-processing techniques, such as sanding, for both BioMed Clear and PEEK materials. The current state is acceptable, but additional smoothing can be performed, when necessary, in other cases.

As anticipated, the permeability tests yielded the expected positive results. Using the same paths and configurations as the current moulds, issues were unlikely, and none arose. The only potential problem area was the design with the pinning mechanism due to cutting through paths. This also proved unproblematic and confirms that the design modifications did not negatively impact permeability. Similarly, dose distribution and capture were as anticipated since the dimensions and catheter specifications were largely unchanged. In clinical settings, catheter placement can be planned and placed accordingly during the design, before use in the operating room.

PEEK could not be utilized during this study due to technical difficulties with the Kumovis R1 printer. Despite developing the design with Biomed Clear, the restrictions imposed by printing with PEEK, such as print direction, were taken into account to ensure that the concept is transferable to PEEK when needed. Transitioning to PEEK would present several challenges. FLM printing with PEEK has larger margins of error compared to resin printers, complicating the fabrication of small joints. Additionally, creating small turns and curves with PEEK might prove difficult, further complicating the design process. However, the previously mentioned optional increase of the margin would help with feasibility, reducing some of these challenges. These limitations mean that while the initial design does consider the unique challenges associated with the Kumovis printer, extensive testing is required to adjust and refine the dimensions and margins of the printed parts.

A consideration in this mould design is the challenge of potential in-vivo assembly. With the pinning system, the catheters guide the mould, simplifying the assembly process. In contrast, the sliding mechanism requires maintaining a fixed sliding angle, which can be difficult without visual guidance. Therefore the feasibility of in-vivo assembly varies depending on the specific case and anatomical location. For instance, in cases like a nasopharynx mould, which is inserted through the mouth and guided by catheters through the nose, visual guidance is minimal, making proper alignment nearly impossible. Additional complications arise from the previously observed looseness due to printer variability. While a looser fit might facilitate assembly, the proposed solution of using Dermabond would not be feasible for in-vivo assembly. In practice, in-vivo assembly holds less significance, as there have been no previous cases where it has caused problems.

The patient specific nature of the moulds remains a general consideration in the proposed method. Despite careful consideration of potential intraoperative changes, there remains a slight possibility of unexpected developments. The success of the mould largely relies on the clinician's estimations. Additionally, no guide is used during the soft tissue resection, increasing the risk of deviating from the planned resection. While this variability cannot be entirely eliminated with the current approach, exploration of surgical navigation techniques may provide more accurate resection. Nevertheless, unforeseen outcomes would present the same challenges.

In addition to exploring surgical navigation techniques, it is also recommended to explore alternatives to the current thermoplastic material. The last time the UMCU investigated such material was in 2019, and given the rapid pace of material innovation, there may now be other suitable options available. The key characteristics to consider would be kneadability, the ability to harden under conditions such as exposure to light, and compatibility with open wounds over multiple days. If such a material is available, it could offer a superior solution to the currently proposed method.

In conclusion, this thesis has successfully developed and tested a method for introducing adaptability into mould design, eliminating the need for thermoplastic materials. While the proposed method shows significant potential, further research is necessary. Addressing the challenges of print variability and PEEK requires implementing and testing the suggested modifications. Future research should additionally focus on evaluating alternative materials that could potentially replace thermoplastics to explore an alternative method.

References

[1] R. C. Hoogeveen, M. L. Hol, B. R. Pieters, B. V. Balgobind, E. W. Berkhout, R. A. Schoot, L. E. Smeele, H. J. Merks, and E. A. Becking, "An overview of radiological manifestations of acquired dental developmental disturbances in paediatric head and neck cancer survivors," *Dentomaxillofacial Radiology*, vol. 49, no. 3, 2020.

[2] A. K. Berthelsen, J. Dobbs, E. Kjellén, T. Landberg, T. R. Möller, P. Nilsson, L. Specht, and A. Wambersie, "What's new in target volume definition for radiologists in ICRU Report 71? How can the ICRU volume definitions be integrated in clinical practice?," *Cancer Imaging*, vol. 7, no. 1, p. 104, 2007.

[3] D. Baltas and N. Zamboglou, "2D and 3D Planning in Brachytherapy," in *New Technologies in Radiation Oncology* (W. Schlegel, T. Bortfeld, and A.-L. Grosu, eds.), pp. 237–254, Berlin, Heidelberg: Springer Berlin Heidelberg, 2006.

[4] G. Barile, A. Leoni, M. Muttillo, R. Paolucci, G. Fazzini, and L. Pantoli, "Fused-Deposition-Material 3D-Printing Procedure and Algorithm Avoiding Use of Any Supports †," pp. 4–6, 2019.

[5] R. A. Schoot, O. Slater, C. M. Ronckers, A. H. Zwinderman, A. J. Balm, B. Hartley, M. W. Van Den Brekel, S. Gupta, P. Saeed, E. Gajdosova, B. R. Pieters, M. N. Gaze, H. C. Mandeville, R. D. Fajardo, Y. C. i. Chang, J. E. Gains, S. D. Strackee, D. Dunaway, C. Abela, C. Mason, L. E. Smeele, J. C. Chisholm, G. A. Levitt, L. C. Kremer, M. A. Grootenhuis, H. Maurice-Stam, C. A. Stiller, P. Hammond, H. N. Caron, and J. H. Merks, "Adverse events of local treatment in long-term head and neck rhabdomyosarcoma survivors after external beam radiotherapy or AMORE treatment," *European Journal of Cancer*, vol. 51, no. 11, pp. 1424–1434, 2015.

[6] B. Vaarwerk, M. L. Hol, R. A. Schoot, W. B. Breunis, M. M. de Win, H. Westerveld, R. D. Fajardo, P. Saeed, M. W. van den Brekel, B. R. Pieters, S. D. Strackee, L. E. Smeele, and J. H. Merks, "AMORE treatment as salvage treatment in children and young adults with relapsed head-neck rhabdomyosarcoma," *Radiotherapy and Oncology*, vol. 131, pp. 21–26, 2 2019.

[7] L. E. Blank, K. Koedooder, H. N. Van Der Grient, N. A. Wolffs, M. Van De Kar, J. H. Merks, B. R. Pieters, P. Saeed, L. Baldeschi, N. J. Freling, and C. C. Koning, "Brachytherapy as part of the multidisciplinary treatment of childhood rhabdomyosarcomas of the orbit," *International Journal of Radiation Oncology Biology Physics*, vol. 77, pp. 1463–1469, 8 2010.

[8] L. E. Blank, K. Koedooder, B. R. Pieters, H. N. van der Grient, M. van de Kar, J. Buwalda, A. J. Balm, J. H. Merks, S. D. Strackee, N. J. Freling, and C. C. Koning, "The AMORE Protocol for Advanced-Stage and Recurrent Nonorbital Rhabdomyosarcoma in the Head-and-Neck Region of Children: A Radiation Oncology View," *International Journal of Radiation Oncology Biology Physics*, vol. 74, pp. 1555–1562, 8 2009.

[9] J. Buwalda, *AMORE (Ablative surgery, MOulage technique brachytherapy and REconstruction) for childhood head and neck rhabdomyosarcoma*. PhD thesis, Universiteit van Amsterdam, 2004.

[10] R. A. Schoot, P. Saeed, N. J. Freling, L. E. Blank, B. R. Pieters, J. N. Van Der Grient, S. D. Strackee, J. Bras, H. N. Caron, and J. H. Merks, "Local Resection and Brachytherapy for Primary Orbital Rhabdomyosarcoma: Outcome and Failure Pattern Analysis," *Ophthalmic Plastic and Reconstructive Surgery*, vol. 32, no. 5, pp. 354–360, 2016.

[11] E. Chen, R. Ricciotti, N. Futran, and D. Oda, "Head and Neck Rhabdomyosarcoma: Clinical and Pathologic Characterization of Seven Cases," *Head and Neck Pathology*, vol. 11, pp. 321–326, 9 2017.

[12] S. X. Skapek, A. Ferrari, A. A. Gupta, P. J. Lupo, E. Butler, J. Shipley, F. G. Barr, and D. S. Hawkins, "Rhabdomyosarcoma," *Nature Reviews Disease Primers*, vol. 5, 12 2019.

[13] N. Suntharalingam, E. B. Podgorsak, and C. H. Tölli, "Brachytherapy: Physical and clinical aspects," in *Radiation Oncology Physics: A Handbook for Teachers and Students*, pp. 451–484, International Atomic Energy Agency (IAEA), 2005.

[14] "3. Definition of Volumes," *Journal of the ICRU*, vol. 14, pp. 55–63, 12 2014.

[15] C. Haie-Meder, R. Pötter, E. Van Limbergen, E. Briot, M. De Brabandere, J. Dimopoulos, I. Dumas, T. P. Hellebust, C. Kirisits, S. Lang, S. Muschitz, J. Nevinson, A. Nulens, P. Petrow, and N. Wachter-Gerstner, "Recommendations from Gynaecological (GYN) GEC-ESTRO Working Group (I): concepts and terms in 3D image based 3D treatment planning in cervix cancer brachytherapy with emphasis on MRI assessment of GTV and CTV," *Radiotherapy and Oncology*, vol. 74, pp. 235–245, 3 2005.

[16] R. Pötter, C. Haie-Meder, E. Van Limbergen, I. Barillot, M. De Brabandere, J. Dimopoulos, I. Dumas, B. Erickson, S. Lang, A. Nulens, P. Petrow, J. Rownd, and C. Kirisits, "Recommendations from gynaecological (GYN) GEC ESTRO working group (II): Concepts and terms in 3D image-based treatment planning in cervix cancer brachytherapy—3D dose volume parameters and aspects of 3D image-based anatomy, radiation physics, radiobiology," *Radiotherapy and Oncology*, vol. 78, pp. 67–77, 1 2006.

[17] M. K. Rooney, D. M. Rosenberg, S. Braunstein, A. Cunha, A. L. Damato, E. Ehler, T. Pawlicki, J. Robar, K. Tatebe, and D. W. Golden, "Three-dimensional printing in radiation oncology: A systematic review of the literature," *Journal of Applied Clinical Medical Physics*, vol. 21, pp. 15–26, 8 2020.

[18] "Using BioMed Clear Resin," 4 2022.

[19] "EXT 220 MED (Kumovis R1)."

[20] Kumovis: a 3D systems company, "Kumovis R1 User Guide," tech. rep., 2021.

[21] E. Miranda, *Moscow Rules: A Quantitative Exposé*. 1 2022.

[22] T. Nilsen, M. Hermann, C. Eriksen, H. Dagfinrud, P. Mowinckel, and I. Kjeken, "Grip force and pinch grip in an adult population: Reference values and factors associated with grip force," *Scandinavian journal of occupational therapy*, vol. 19, pp. 288–296, 6 2011.

A

Appendix

A.1 Exact dose volume parameters

Table 11: Exact values of the dose volume parameters illustrated in the boxplots

	Median	Mean	Min	Max
%V150 outside mould	18.23	22.12	3.18	54.70
%V200 outside mould	11.24	15.82	5.01	40.49
D90 (cGy)	126.78	125.21	112.64	136.57
D98 (cGy)	113.66	111.45	101.79	116.08

A.2 Performed testing for dimension and margin

A.2.1 Test 1

In the first test, two sets of cubes were printed to evaluate multiple facets of the coupling system. The primary difference between the two sets was the dimension of the extruding part, which extended either 2 mm or 3 mm. Each set consisted of an extruding cube (featuring extruding parts of varying lengths, as well as pins of different lengths and diameters) and a corresponding intruding cube (with slots corresponding to the extruding parts, varying in margin). The exact measurements of these test cubes can be found in Figure 16, 17, 18 and 19.

The combinations were then assessed based on the following criteria (Table 12):

- *'Stays together'* - The system could be assembled and would consequently not fall apart.
- *'No rotation'* - There was no possible rotation within the mould.
- *'Material use'* - The system did not use an excessive amount of material and was not larger than necessary.
- *'Space in mould'* - The mechanism could realistically fit inside a clinical mould.

Conclusions:

Sliding mechanism

- The coupling mechanism should occupy only 2 mm of space to accommodate catheter paths and the potential for even smaller moulds.
- A 0.1 margin works well for the 2 mm extrusion.
- Mechanisms with 5 mm and 10 mm lengths exhibited potential rotation at the top, suggesting that a longer mechanism would be more stable.
- A longer mechanism resulted in a tighter fit due to increased friction.
- However, a longer mechanism would also require more material.
- The pinning mechanism could not be tested in this design due to an error, but it was observed that the 0.1 mm margin was too large and did not hold the parts together.

Pinning mechanism

- The pinning mechanism could not be tested in this design due to an error, but it was observed that the 0.1 mm margin was too large and did not hold the parts together.

Table 12: Results from prototyping test 1

	Stays together	No rotation	Material use	Space in mould
Sliding mechanism 2mm				
30mm long, margin 0	✕	-	✕	✓
30mm long, margin 0.1	✓	✓	✕	✓
30mm long, margin 0.2	✕	-	✕	✓
30mm long, margin 0.3	✕	-	✕	✓
20mm long, margin 0	✕	-	✕	✓
20mm long, margin 0.1	✓	✓	✕	✓
20mm long, margin 0.2	✕	-	✕	✓
20mm long, margin 0.3	✕	-	✕	✓
10mm long, margin 0	✕	-	✓	✓
10mm long, margin 0.1	✓	✕	✓	✓
10mm long, margin 0.2	✕	-	✓	✓
10mm long, margin 0.3	✕	-	✓	✓
5mm long, margin 0	✕	-	✓	✓
5mm long, margin 0.1	✓	✕	✓	✓
5mm long, margin 0.2	✕	-	✓	✓
5mm long, margin 0.3	✕	-	✓	✓
Sliding mechanism 3mm				
30mm long, margin 0	✕	-	✕	✕
30mm long, margin 0.1	✓	✓	✕	✕
30mm long, margin 0.2	✕	-	✕	✕
30mm long, margin 0.3	✕	-	✕	✕
20mm long, margin 0	✕	-	✕	✕
20mm long, margin 0.1	✓	✓	✕	✕
20mm long, margin 0.2	✕	-	✕	✕
20mm long, margin 0.3	✕	-	✕	✕
10mm long, margin 0	✕	-	✓	✕
10mm long, margin 0.1	✓	✕	✓	✕
10mm long, margin 0.2	✕	-	✓	✕
10mm long, margin 0.3	✕	-	✓	✕
5mm long, margin 0	✕	-	✓	✕
5mm long, margin 0.1	✓	✕	✓	✕
5mm long, margin 0.2	✕	-	✓	✕
5mm long, margin 0.3	✕	-	✓	✕

Figure 16: Technical drawing of the test cube with the 2 mm extruding part

The following labels appear on the drawing:

A: height=1, Ø=2
B: heigth=1.5, Ø=2
C: height=1.5, Ø=4
D: height=2, Ø=2

Dept. | Technical reference | Created by: Sanne Hodes | Approved by
Document type | Document status
Title: 2mm extruding part | DWG No.
Rev. | Date of issue | Sheet 1/1

The technical drawing contains the following labels and annotations:

- 30
- Margin=0
- Margin=0.1
- Margin=0.2
- Margin=0.3
- A, B, C, D, E, F, G, H, I, J, K, L
- 2

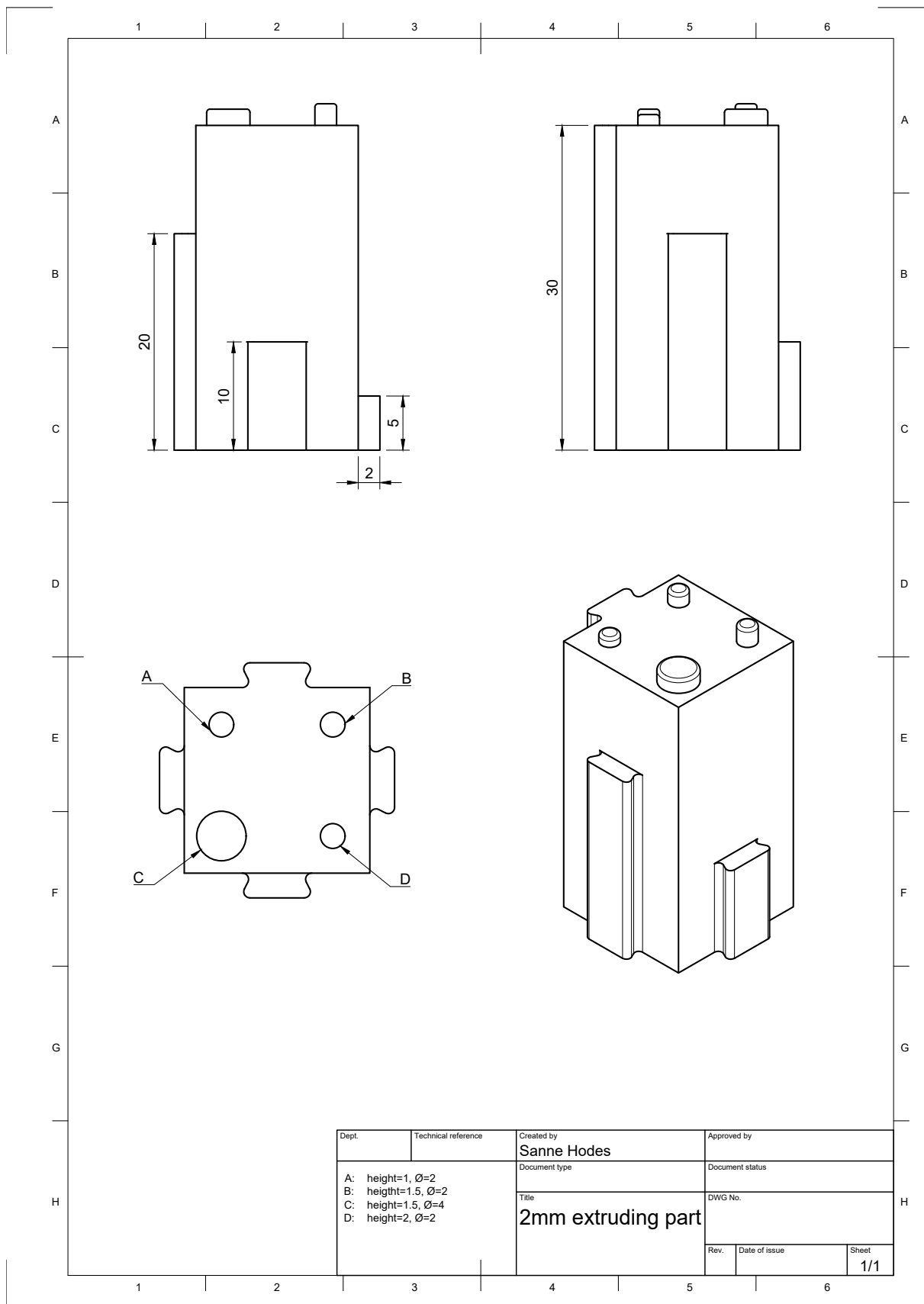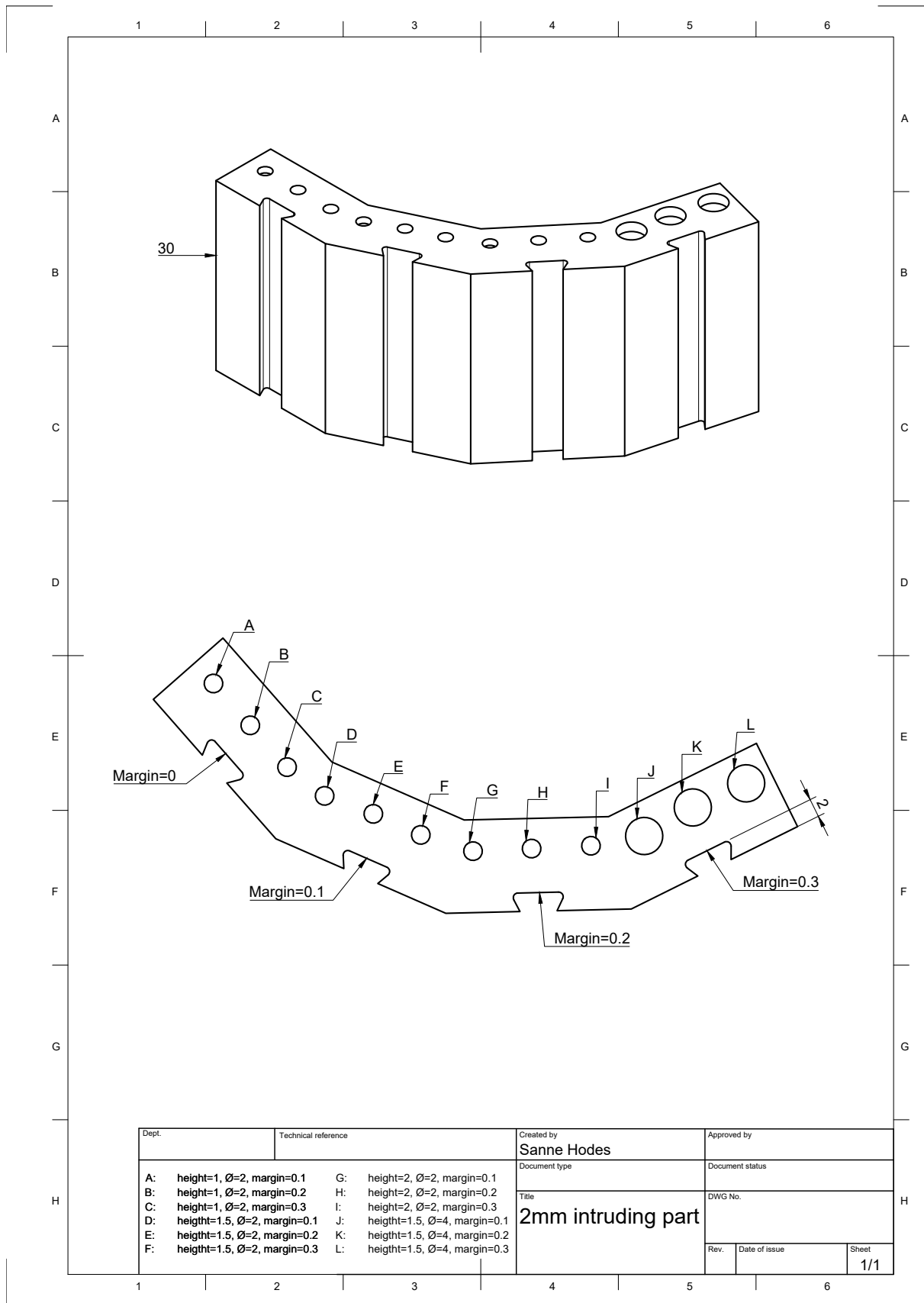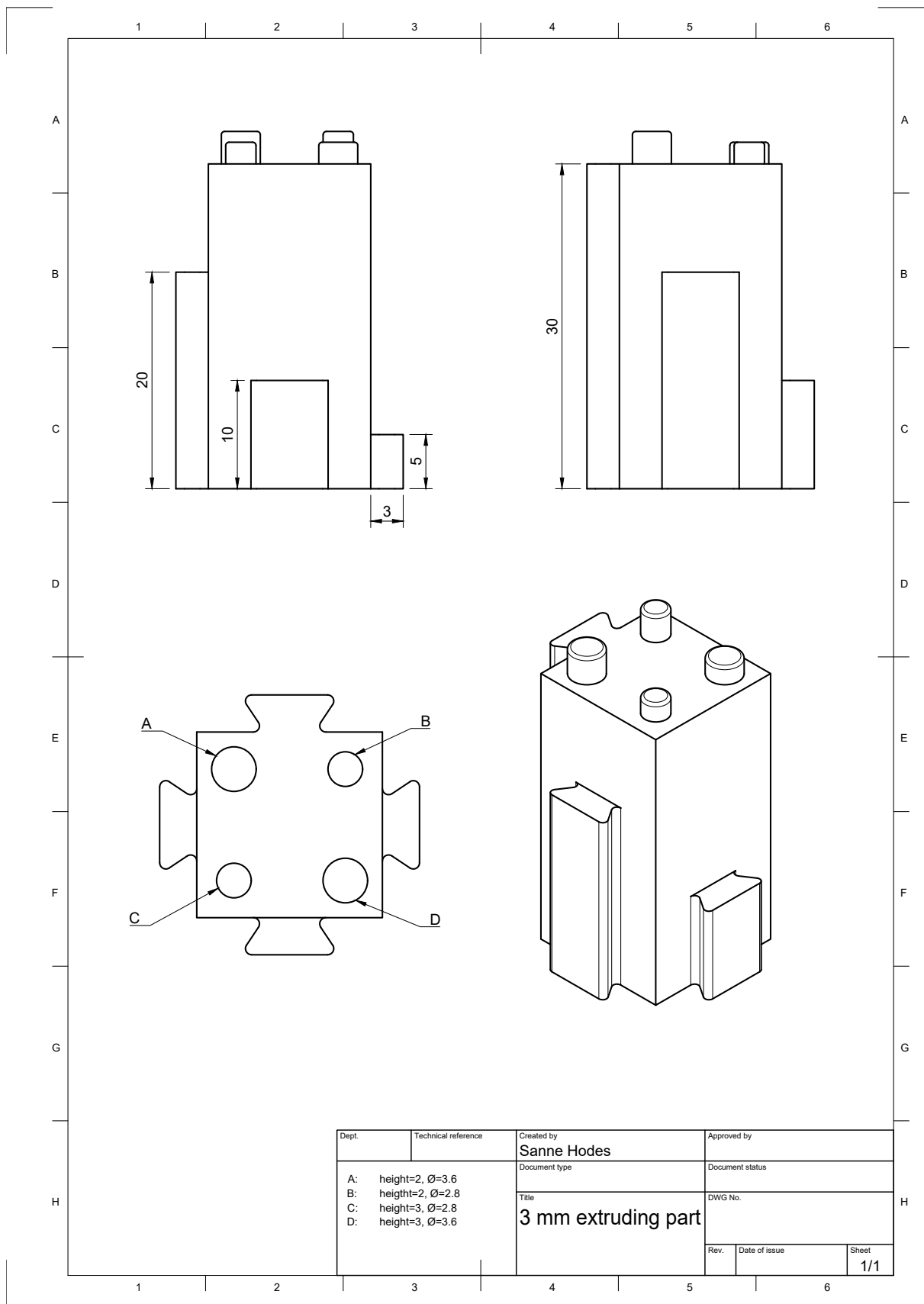| Dept.		Technical reference		Created by	Approved by	
				Sanne Hodes		
				Document type	Document status	
A:	height=1, Ø=2, margin=0.1	G:	height=2, Ø=2, margin=0.1			
B:	height=1, Ø=2, margin=0.2	H:	height=2, Ø=2, margin=0.2	Title	DWG No.	
C:	height=1, Ø=2, margin=0.3	I:	height=2, Ø=2, margin=0.3	2mm intruding part		
D:	heigtht=1.5, Ø=2, margin=0.1	J:	heigtht=1.5, Ø=4, margin=0.1			
E:	heigtht=1.5, Ø=2, margin=0.2	K:	heigtht=1.5, Ø=4, margin=0.2		Rev.	Date of issue	Sheet
F:	heigtht=1.5, Ø=2, margin=0.3	L:	heigtht=1.5, Ø=4, margin=0.3			1/1

Figure 17: Technical drawing of the test cube with the 2 mm intruding part

Figure 18: Technical drawing of the test cube with the 3 mm extruding part

30

Margin=0

A
B
C
D
E
F
G
H
I
J
K
L

3

Margin=0.1

Margin=0.2

Margin=0.3

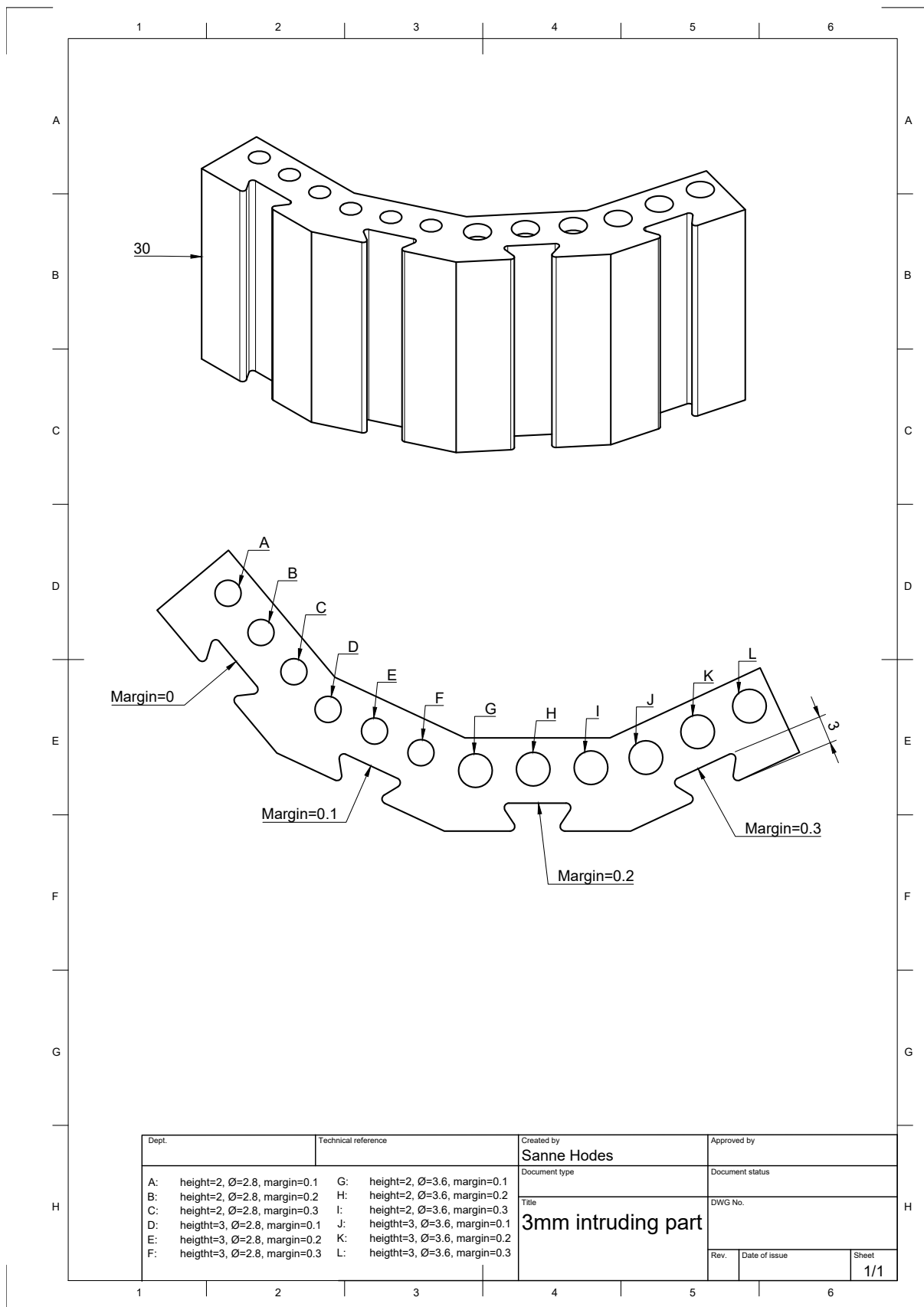| Dept.		Technical reference		Created by		Approved by	
				Sanne Hodes			
A: height=2, Ø=2.8, margin=0.1	G: height=2, Ø=3.6, margin=0.1			Document type		Document status	
B: height=2, Ø=2.8, margin=0.2	H: height=2, Ø=3.6, margin=0.2						
C: height=2, Ø=2.8, margin=0.3	I: height=2, Ø=3.6, margin=0.3			Title		DWG No.	
D: heigtht=3, Ø=2.8, margin=0.1	J: heigtht=3, Ø=3.6, margin=0.1			3mm intruding part			
E: heigtht=3, Ø=2.8, margin=0.2	K: heigtht=3, Ø=3.6, margin=0.2						
F: heigtht=3, Ø=2.8, margin=0.3	L: heigtht=3, Ø=3.6, margin=0.3					Rev. Date of issue Sheet 1/1	

Figure 19: Technical drawing of the test cube with the 3 mm intruding part

A.2.2 Test 2

Building upon the sliding mechanism tests conducted in the first trial, the second test was done to minimize material usage while addressing the rotation issue. A joint with two mechanisms positioned on opposite sides was developed, maintaining a joint length of 5 mm and depth of 2 mm. Two identical cubes were created to repeat the margin test, hypothesizing that increased friction might influence the results. The exact measurements of this test cube can be found in Figure 20.

Conclusions:

- The 0.1 mm margin was found to be suitable.

- This design will be implemented and further evaluated in a clinical case to assess its performance and suitability for practical use.

A.2.3 Test 3

In the third round of testing, focus was placed on further refining the pinning mechanism. Following the observation in the initial test that even a 0.1 mm margin failed to secure the parts together effectively, a tapered design was introduced. Maintaining the constraint that the joint should not exceed 2 mm in depth, variations in taper extent, diameters, and margins were explored. The exact measurements of these test cubes can be found in Figure 21 and 22.

Conclusions:

- Differences in diameter were found to have negligible impact; therefore, the smaller diameter was chosen to optimize space within the mould.

- A margin of 0.05 mm was determined to be optimal. The smaller margin did not extend far enough, leaving a small air gap between the parts.

A.2.4 Test 4

In the fourth and final testing round, the dimensions and margins of the pinning mechanism were confirmed to be appropriate for implementation the clinical case. However, issues arose with the sliding mechanism, which proved too tight to function properly. Attempts to force the mechanism together resulted in segments becoming stuck. It was hypothesized that the increased dimensions of the cutting plane in the clinical mould compared to the testing cube resulted in increased friction, rendering the initial dimensions inadequate.

To address this issue, an additional 0.1 mm margin was added to the cutting plane. Despite this adjustment, the margin was still insufficient. Subsequently, margins of 0.15 mm and 0.2 mm were tested. The 0.2 mm margin was too big, whereas the 0.15 mm margin achieved functionality.
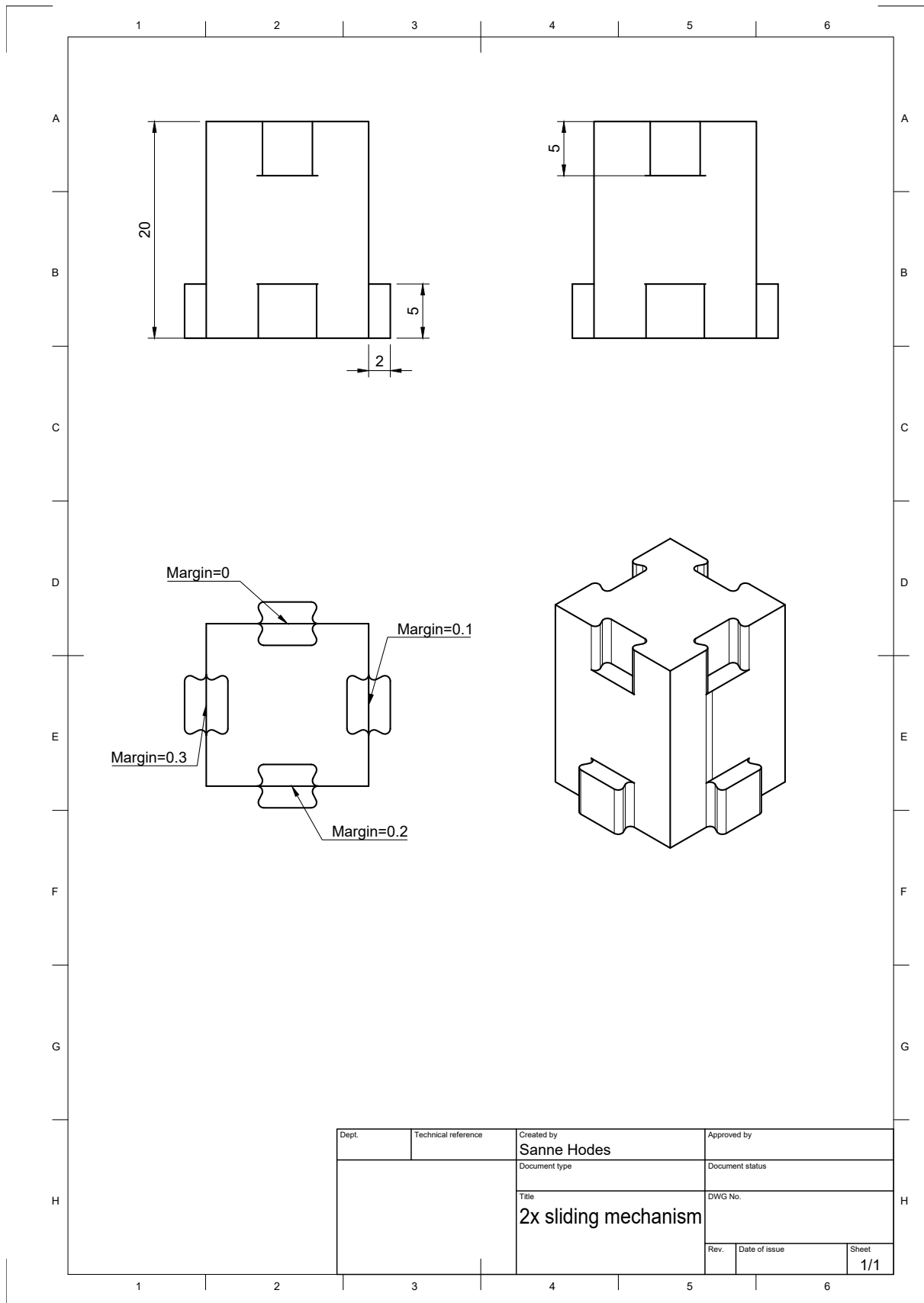
Figure 20: Technical drawing of the test cube with two times the sliding mechanism with the 2 mm extruding part
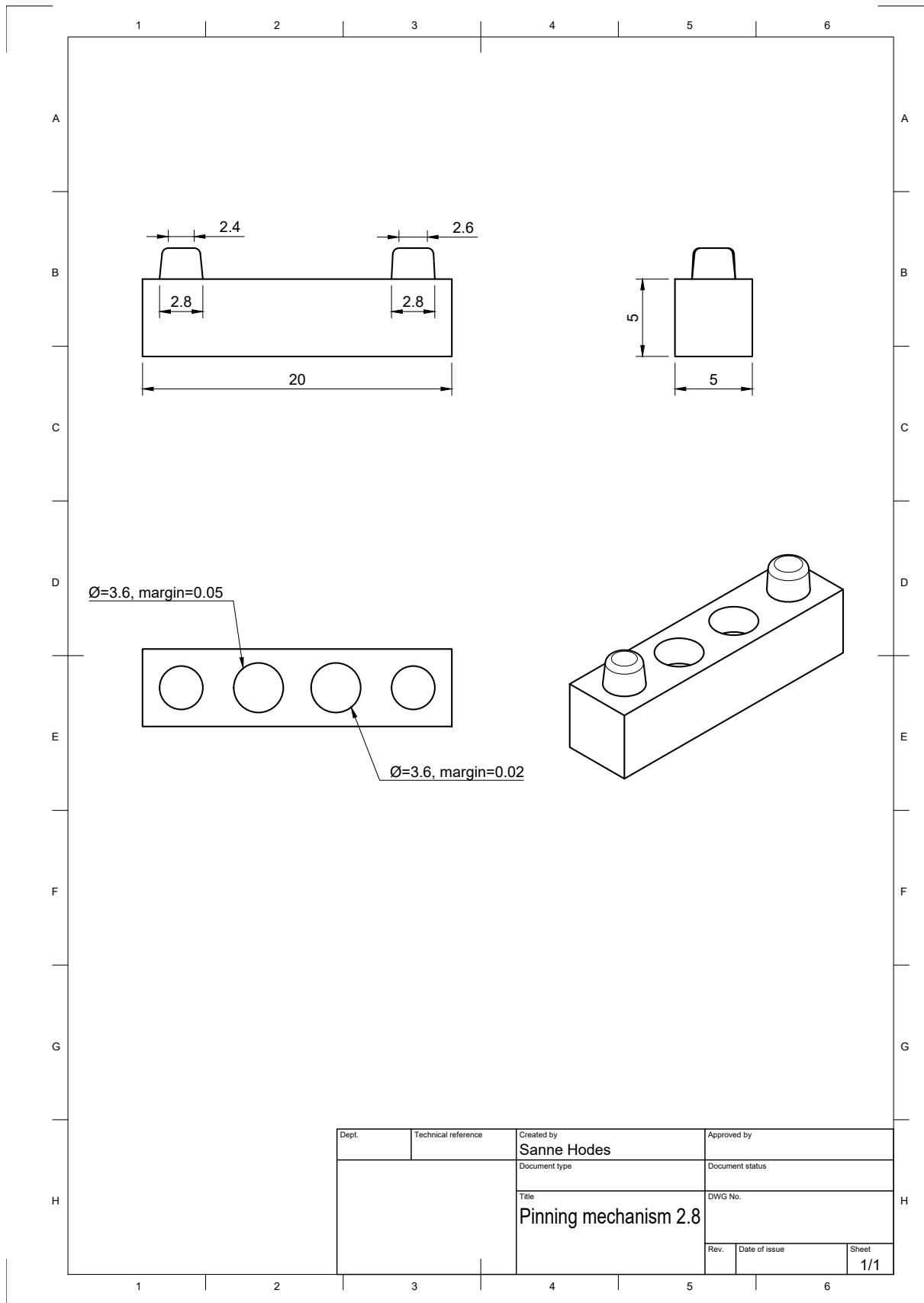
Figure 21: Technical drawing of the test cube for the pinning mechanism with the smaller pins
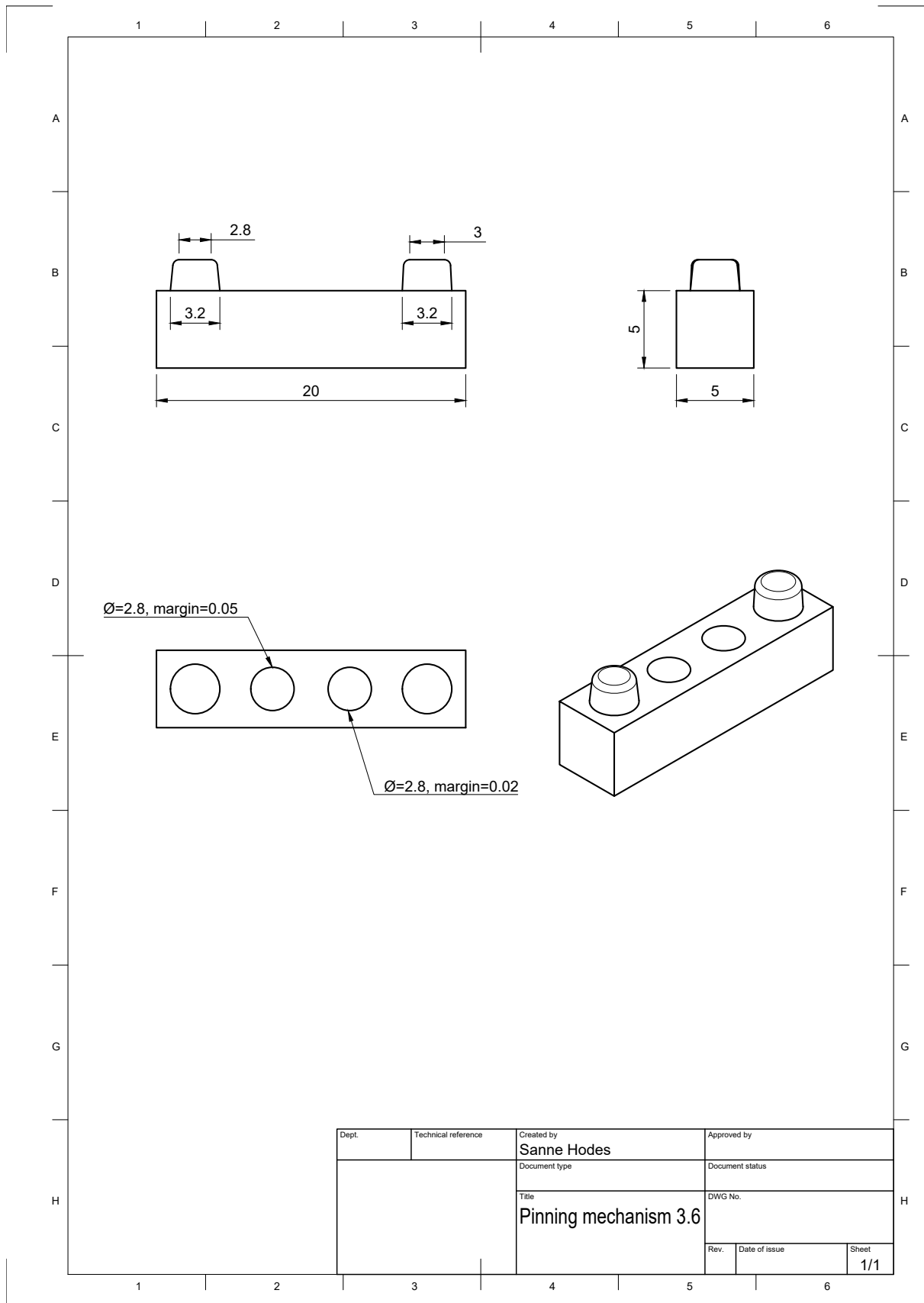
Figure 22: Technical drawing of the test cube for the pinning mechanism with the larger pins

A.3   Results of the reprint of the sliding mechanism

Table 13: Results of the test conducted on reprint of the mould design with sliding mechanism regarding the strength and firmness of the connection

Sliding mechanism (reprint)

Mechanism strength

	Holds 30N	Max tested		Holds 30N	Max tested
1+3	✓	50N	2+3	✓	50N
1+4	✓	50N	2+4	✓	50N
1+5	✓	50N	2+5	✓	50N
1+6	✓	50N	2+6	✓	50N

Firmness connection

	Force (g)	Force (N)		Force (g)	Force (N)
1+3	1100	10.8	2+3	110	1.1
1+4	2300	22.6	2+4	300	2.9
1+5	520	5.1	2+5	20	0.2
1+6	310	3.0	2+6	85	0.8